"Studying of the Color(constituent) Quark Condensate (CQC) with the light ion beams"
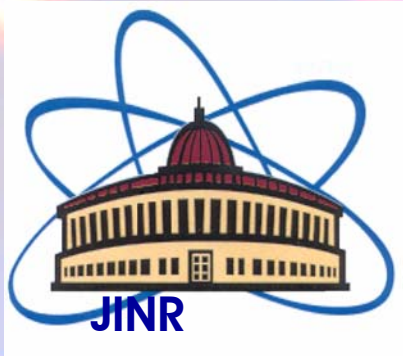
S.S. Shimanskiy (JINR, Dubna)

In Russia there are two accelerators to perform baryon matter investigations (Dubna and Protvino).

Some time in future will be two new projects – JPARC(Japan) and FAIR(Germany).

JINR

Veksler & Baldin
Laboratory of High
Energies
Dubna

NUCLOTRON

Beams	Intensity (particles per cycle)	
	available now	next step
p	$2.5 \cdot 10^{10}$	10^{13}
d	$5 \cdot 10^{10}$	10^{13}
d↑	$3 \cdot 10^8$	$5 \cdot 10^{10}$
^{4}He	$8 \cdot 10^8$	$2 \cdot 10^{12}$
^{7}Li	$2 \cdot 10^9$	$5 \cdot 10^{12}$
^{10}B	$2 \cdot 10^7$	10^{10}
^{12}C	$6.5 \cdot 10^8$	$2 \cdot 10^{12}$
^{24}Mg	$1.2 \cdot 10^8$	$5 \cdot 10^{11}$
^{40}Ar	10^8	10^{10}
^{56}Fe	10^6	10^{11}
^{84}Kr	10^3	$5 \cdot 10^8$

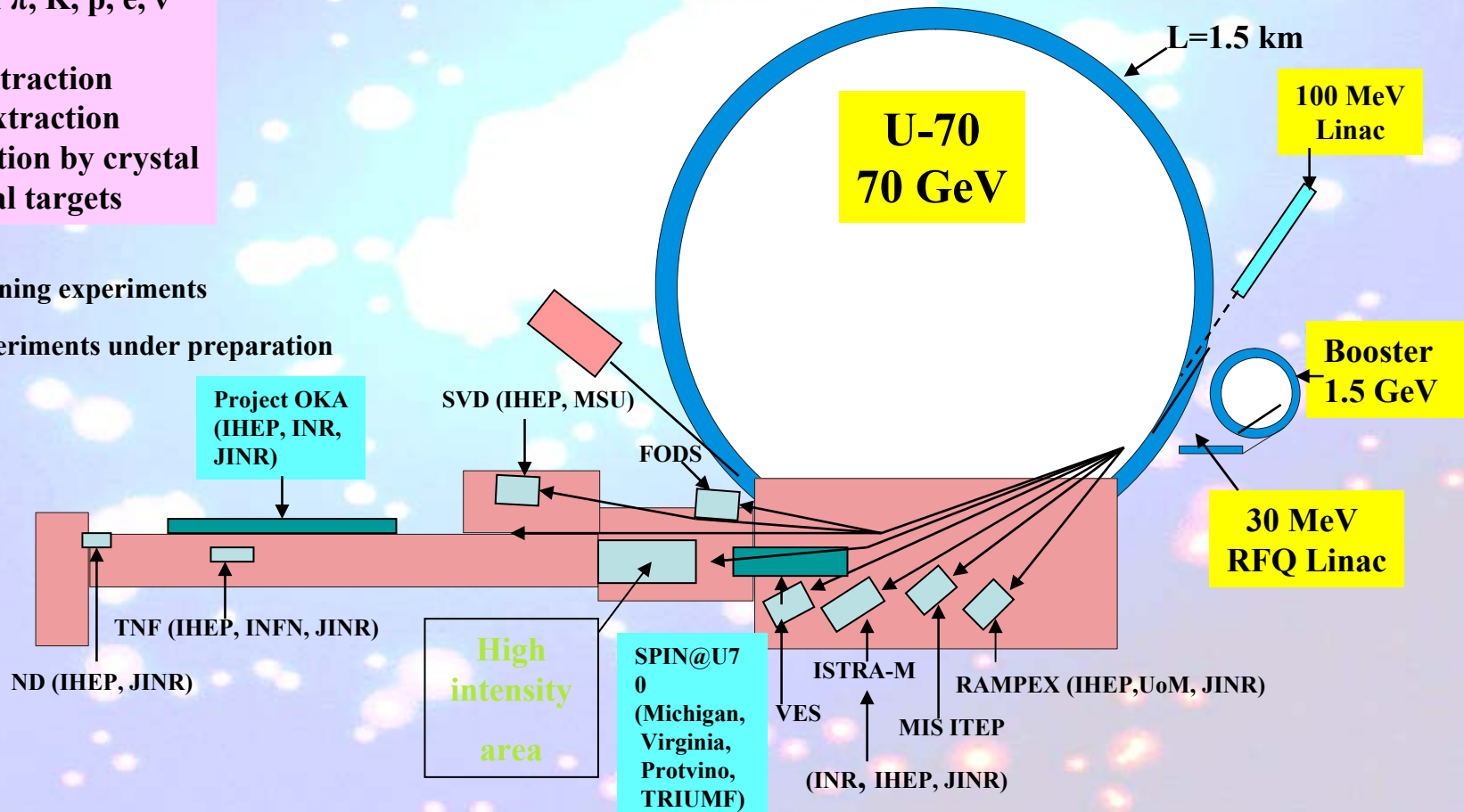## LAYOUT OF IHEP EXPERIMENTAL AREA

E=70 GeV,
I=1.7•10^{13} ppp
Beams of π, K, p, e, ν

- Fast extraction
- Slow extraction
- Extraction by crystal
- Internal targets

☐ - Running experiments

☐ - Experiments under preparation

L=1.5 km

U-70 70 GeV

100 MeV Linac

Booster 1.5 GeV

30 MeV RFQ Linac

Project OKA (IHEP, INR, JINR)

SVD (IHEP, MSU)

FODS

TNF (IHEP, INFN, JINR)

ND (IHEP, JINR)

High intensity area

SPIN@U70 (Michigan, Virginia, Protvino, TRIUMF)

VES

ISTRA-M

MIS ITEP

RAMPEX (IHEP,UoM, JINR)

(INR, IHEP, JINR)

Program of DUBNA-SPIN-07

DSPIN'07

	03.09 Mo	04.09 Tu	05.09 We	06.09 Th	07.09 Fr
Chair	*Lednicky*	*Bressan*	*Soffer*	*Belostotski*	*GrossePerdekamp*
9.30	OPENING	Belostotski	Bunce	Grosse Perdekamp	Crabb
9.50	Soffer				
10.10		Korotkov	Dunlop	Artru	Alekseev
10.30	Bressan				Bogdanov
10.50		Borissov	Dodge	Ladygin	Nurushev
11.10	Teryaev				Runtso
11.30 11.50	*Coffee break*	*Coffee break*	*Coffee break*	*Coffee break*	*Coffee break*
Chair	*Borissov*	*Savin*	*Bedfer*	*Piskunov*	*Nikolaev*
11.50	Santos	Varanda (30')	Kubarovsky	Kurilkin P.	Okorokov
12.10		Veretennikov (30')		Kurilkin A.	Naumov
12.30	Bedfer		Ermolaev	Vasiliev T.	Abramov
12.50		Prokudin		Kiselev A.	Alikhanov
13.10	Klimaszewski		O'Brien	Morozov	Chen
13.30 15.00	*Lunch*	*Lunch*	*Lunch*	*Lunch*	*Lunch*
Chair	*Nassalski*	*d'Hose*	*Ginzburg*	*Zulkarneev*	*Ramsey*
15.00	d'Hose	Vilardi (30')	Hoek	Sharov	Jenkovszky
15.20		Goloskokov		Shindin	Vasiliev A.
15.40	Sivers	Mueller	Nikolaev	Strunov	
16.00		Ivanov D.		Azhgirey	Tikhonin
16.20 16.40	*Coffee break*	*Coffee break (10')*	*Coffee break*	*Coffee break*	*Coffee break*
Chair	*Sandacz*	*Teryaev*	*Mueller*	*Miklukho*	*Dodge*
16.40	Savin	Dorokhov	Troshin	Shimanskiy	Pankov
17.00	Wakamatsu	Ivanov I.	Isayev	Gerasimov	Koerner
17.20	Ramsey	Meissner	Cherednikov	Lykasov	Ginzburg
17.40	Sidorov	Kivel	Pasechnik	Lyuboshitz	Studenikin
18.00	Simolo	Ramilli	Burinskii	Silenko	Soffer, summary
18.20	Christova	Selyugin	Chernitskii	Huseynov	
18.40	Kotikov	Ivanov O.			*Farewell party*
19.00	*Welcome Party*		*Concert*	*Conference dinner*	

Parallel sessions

	03.09 Mo	04.09 Tu	05.09 We	06.09 Th	07.09 Fr
Chair		*Ladygin*	*Crabb*		
16.40		Miklukho	Kiselev Yu.		
17.00		Svirida	Plis		
17.20		Uzikov	Pivovarov		
17.40		Nikolenko	Filatov		
18.00		Chetvertkova	Musulmanbekov		
18.20		Shikhalev			
18.40					*Farewell party*
19.00	*Welcome Party*		*Concert*	*Conference dinner*	

Spin Physics at Nuclotron
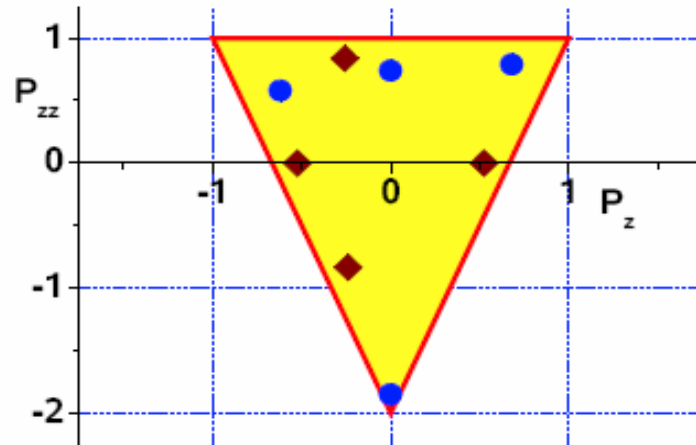
V.P.Ladygin et al. (on behalf of LHE SPIN group)

Seminar LNP-JINR, 12 December 2007

Content of the talk

- Introduction

- Review of the current status of spin physics at LHE

- Future plans for Nuclotron

- Spin physics at NICA

- Conclusions

The results given in the talk were provided by

L.S.Azhgirey, V.V.Glagolev, V.I.Sharov, N.M.Piskunov, L.N.Strunov, L.S.Zolin, P.K.Kurilkin, M.A.Shikhalev, V.A.Krasnov, N.B.Ladygina, S.S.Shimansky

PHYSICAL PROGRAMM AND ACCELERATION OF POLARIZED LIGHT NUCLEI BEAMS AT JINR NUCLOTRON

S. Vokal[1], A.D. Kovalenko[1], A.M. Kondratenko[2], M.A. Kondratenko[2], V.A. Mikhailov[1], Yu.N. Filatov[1] and S.S. Shimanskiy[1†]

(1) *JINR, Dubna, Russia* , (2) *TPO "Zaryad", Novosibirsk, Russia*
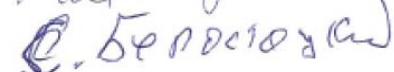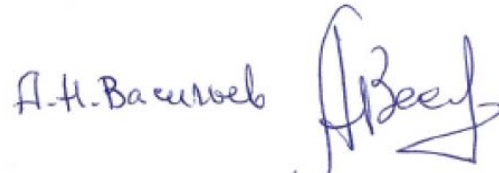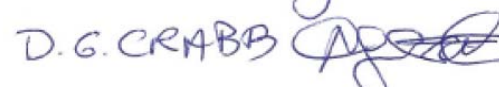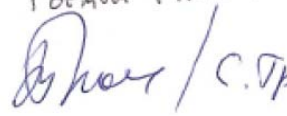† *E-mail: shimanskiy@jinr.ru*
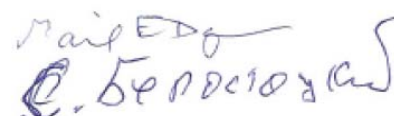
Abstract

The physical spin program at high p_T region and energies $s_{NN}^{1/2} \sim 10 \; GeV$ is discussed. It's shown that cumulative processes, color transparency problem and polarization phenomenons directly connect with properties new form of the nuclear matter as Color Quark Condensate(CQC). Studies of CQC one of the most important physical problem and can be realized using polarized ion beams at JINR nuclotron-M (and in future at NICA). The calculations of spin resonance strengthes in the linear approximation for p, d, t and ^3He beams in the JINR nuclotron are presented. The methods to preserve the degree of polarization during crossing the spin resonances are examined. The method of matching the direction of polarization vector during the beam injection in to the ring of the nuclotron is given. These methods of spin resonance crossing can be used to accelerate polarized beams in the other cyclic accelerators.

XII Advanced research Workshop on High Energy Spin Physics
(DUBNA-SPIN-07)

The spin physics attracts great attention since the 70th when at the energy of ns ~ 10 GeV. In reactions with hadrons in complete contradiction with ictions of QCD that polarization characteristics must disappear at high gies the huge spin effects were discovered. The begun detailed studies with the er energies showed that the observed spin effects do not disappear even at gies of hundreds GeV. The deep inelastic lepton scattering on polarized targets 0th and 90th of the past century led to the problem named "spin crisis". Until the spin effects have not found complete physical explanation in the ework of QCD. The situation when there is no adequate understanding of rization phenomena at the energies ~ 10 GeV is real challenge to nowadays retical models. This energy region becomes especially important in connection the increasing interest to the astrophysical problems, where enormous netic fields up to ~ 10^{18} Gs have been discovered. Strong magnetic fields can s indication to an enormous role of the spin effects in processes of the massive evolution, the nucleosynthesis of heavy elements and the solution of the tery of the supernova explosions. One of the most important problem for high-gy physics remains until now is understanding the nature of the spin and, in icular, skill to calculate the spin of hadrons from constituent spins.

In the program of the international conference DSPIN07 the results of ivity with polarized beams of the LHE JINR accelerator complex have been ented. These reports have reflected: the development of new methods to ervation of polarization in the nuclotron for polarized protons and the lightest ei; the project to create new polarized ions source (in plan to use components n IUCF CIPIOS source); the proposals of further spin research with polarized ns of modernized nuclotron-M and in a future with NICA-collider beams. All e proposals are actually the substantiation of the project for creation on tron-M the center for spin studies in the region of energies ~ 10 GeV. The eleration of the lightest polarized nuclei will make possible for the first time ies of the polarized nuclear matter collisions (d↑d↑, d↑^{3}He↑ and ^{3}He↑^{3}He↑), he first time study of the complete set of the isotopic states of the nucleon-eon interactions (p↑p↑, n↑p↑ and n↑n↑) and study of the of orbital angular mentum contribution to the nucleon spin. Accelerator complex with such ibilities will not have a concurrence from other activities which will lead rization studies and obtained data will help to resolve the riddles of the spin, ch do not have the solution since 70th. Materials which have been presented on PIN07 confirm high level and urgency of JINR polarization studies and the oubted realizability of the proposed project of creation of a unique center for rization studies. Spin community (presented on DSPIN07) expresses their plete interest in realization of polarization project on nuclotron-M and future elopment the spin program on NICA-collider.

1. **Bunce Gerry** (BNL, Brookhaven, USA)
2. **Soffer Jacques** (Temple Univ. Philadelphia, USA)
3. **Belostotski Stanislav** (PNPI, Gatchina, Russia)
4. **Dodge Gail** (Old Dominion Univ. Norfolk, USA)
5. **Sivers Dennis** (Portland Phys. Inst. USA)
6. **Vasiliev Alexander** (IHEP, Protvino, Russia)
7. **Ramsey Gordon** (Loyola Univer. Chicago, USA)
8. **Crabb Donald G.** (Univ. of Virginia, Charlottesville, USA)
9. **Troshin Sergey** (IHEP, Protvino, Russia)
10. **Nurushev Sandibek** (IHEP, Protvino, Russia)
11. **Ginzburg Ilja** (IMSBRAN Novosibirsk, Russia)
12. **Grosse Perdekamp Matthias** (Univ. of Illinois, Upton, USA)

We can see the CQC phase in ordinary nuclear mater and highlight this state in pA- and AA-collisions. This state directly connected with properties of the core for NN-interaction. We don't know well NN-interaction in overlapping range.

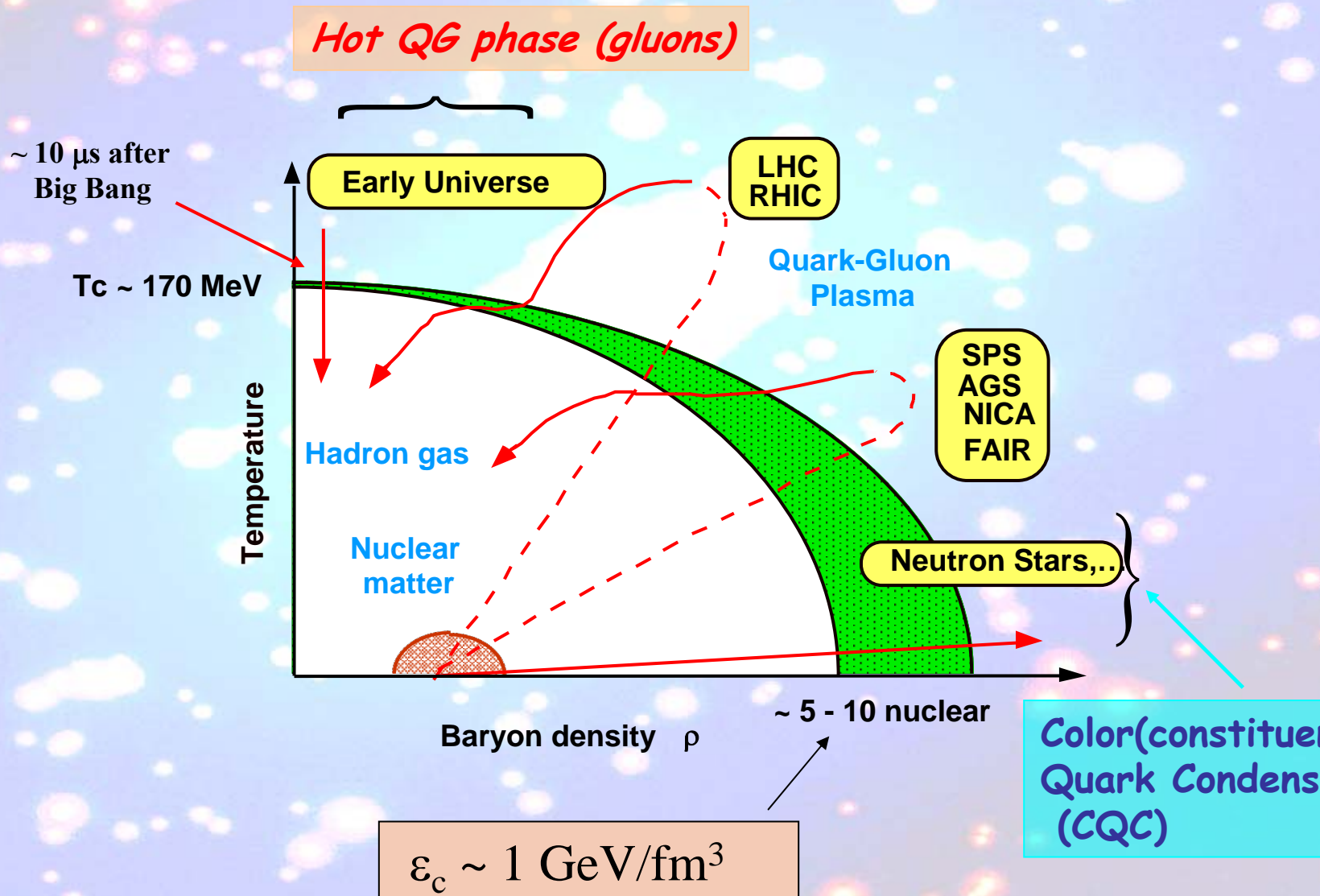# Let us look at the nucleon-nucleon interaction:

- Deuteron is weakly bound
- Large radius
- di-neutron and di-proton unbound
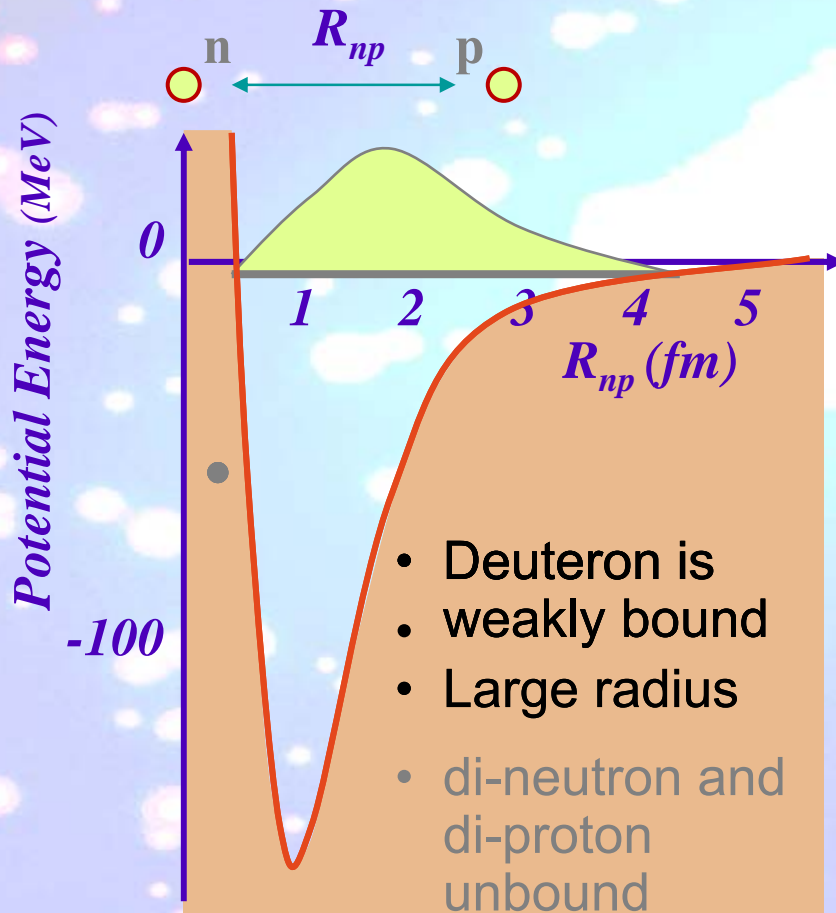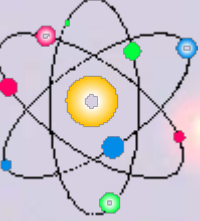
Deuteron static properties

Таблица 1: Статические свойства дейтрона

	$E_D(MeV)$	$P_D(\%)$	$< r_D^2 >^{1/2} (fm)$	$Q(fm^2)$	$\eta = \frac{A_D}{A_S}$	$f_{\pi NN}^2$	$\mu_D(n.m)$
Exp.	2.224579(9)	—	1.9560(68)	0.2859(3)	0.0271(4)	0.0776(9)	0.857406(1)
MU	2.2246	6.78	1.9611	0.2860	0.0271	0.07745	0.843
Paris	2.2250	5.77	1.9716	0.2789	0.0261	0.078	0.853
RHC	2.2246	6.50	1.9602	0.2770	0.0259	0.0757	0.840
RSC	2.2246	6.47	1.9569	0.2796	0.0262	0.0757	0.843
Bonn	2.225	4.58	1.86	0.2856	0.0267	—	—

Table 1: Deuteron properties in the dressed bag model.

Model	E_d(MeV)	$P_D(\%)$	r_m(fm)	Q_d(fm^2)	μ_d (μ_N)	A_S(fm$^{-1/2}$)	$\eta(D/S)$
RSC	2.22461	6.47	1.957	0.2796	0.8429	0.8776	0.0262
Moscow 99	2.22452	5.52	1.966	0.2722	0.8483	0.8844	0.0255
Bonn 2001	2.224575	4.85	1.966	0.270	0.8521	0.8846	0.0256
DBM (1) $P_{in} = 3.66\%$	2.22454	5.22	1.9715	0.2754	0.8548	0.8864	0.0259
DBM (2) $P_{in} = 2.5\%$	2.22459	5.31	1.970	0.2768	0.8538	0.8866	0.0263
experiment	2.224575		1.971	0.2859	0.8574	0.8846	0.0263

QCD phase diagram

Hot QG phase (gluons)

~ 10 μs after Big Bang

Early Universe

LHC RHIC

Quark-Gluon Plasma

Tc ~ 170 MeV

SPS AGS NICA FAIR

Hadron gas

Temperature

Nuclear matter

Neutron Stars,..

Baryon density ρ

~ 5 - 10 nuclear

Color(constituent) Quark Condensate (CQC)

$$\varepsilon_c \sim 1 \ GeV/fm^3$$

RHIC Physics: 3 Lectures

Larry McLerran

Physics Department PO Box 5000 Brookhaven National Laboratory Upton, NY 11973 USA

September 13, 2003

The Evolving QCD Phase Transition

t ~ 1980

Critical Temperature 150 - 200 MeV $(\mu_B = 0)$
Critical Density 1/2-2 Baryons/Fm^3 $(T=0)$

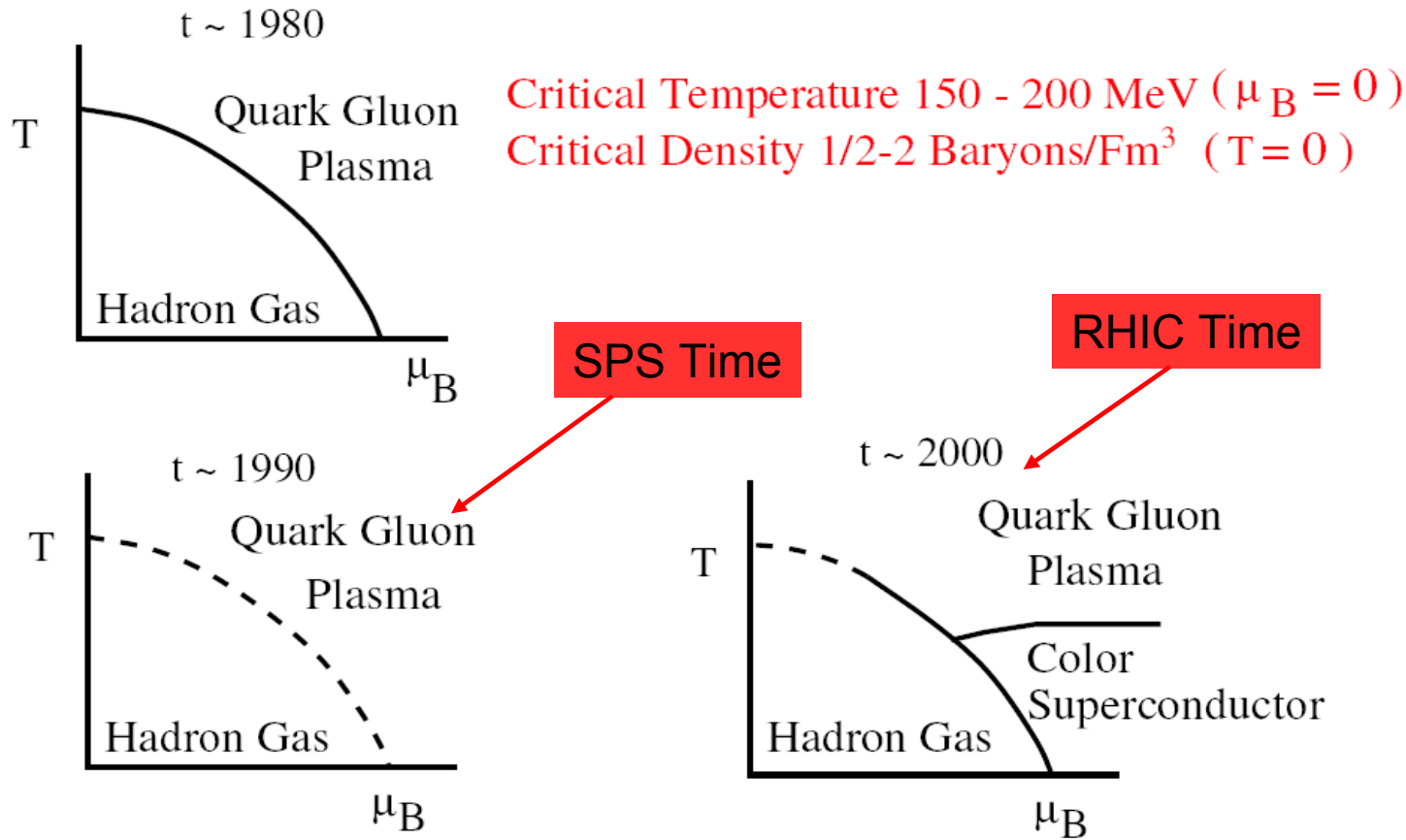SPS Time

RHIC Time

t ~ 1990

t ~ 2000

Figure 4: A phase diagram for QCD collisions.

What if we compress/heat the system so much that the individual hadrons start to interpenetrate?

II. Way for Hot
QG phase

Heavy AA-collisions

1. QGP, sQGP, CGC,
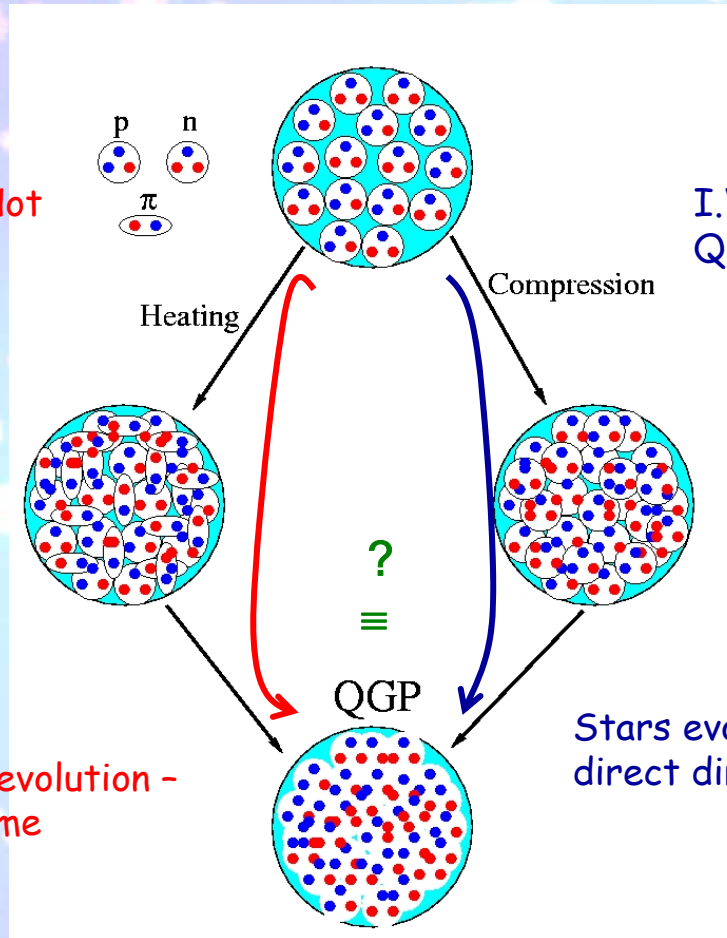   GLAZMA or …
2. Early time of Universe
   evolution

Universe evolution –
back in time

I. Way for Cold
QG phase

Cumulative and high p_T physics

1. Multiquarks states in the cold
   nuclear matter or …
2. Properties of the multiquarks
   states, high density states
3. Stars evolution, dark matter

Stars evolution -
direct direction

Final phases will be equal or not?

DOLIN WEBER,* ALEXANDER HO! RODRIGO P. NEGREIROS‡
PHILIP ROSENFIELD§

$H \sim 10^{17}$ Gs

$E \sim 10^{19}$ V/cm

quark-hybrid star

traditional neutron star

hyperon star

neutron star with pion condensate

N+e
N+e+n
n,p,e, μ
n,p,e, μ

superconducting protons

n superfluid

u,d,s quarks
2SC
CFL

Σ,Λ,Ξ,Δ H

π⁻

K⁻

crust

Fe

10^{6} g/cm^3
10^{11} g/cm^3
10^{14} g/cm^3

Hydrogen/He atmosphere

color−superconducting strange quark matter (u,d,s quarks)

2SC
2SC+s

CFL
CFL−K⁺
CFL−K⁰
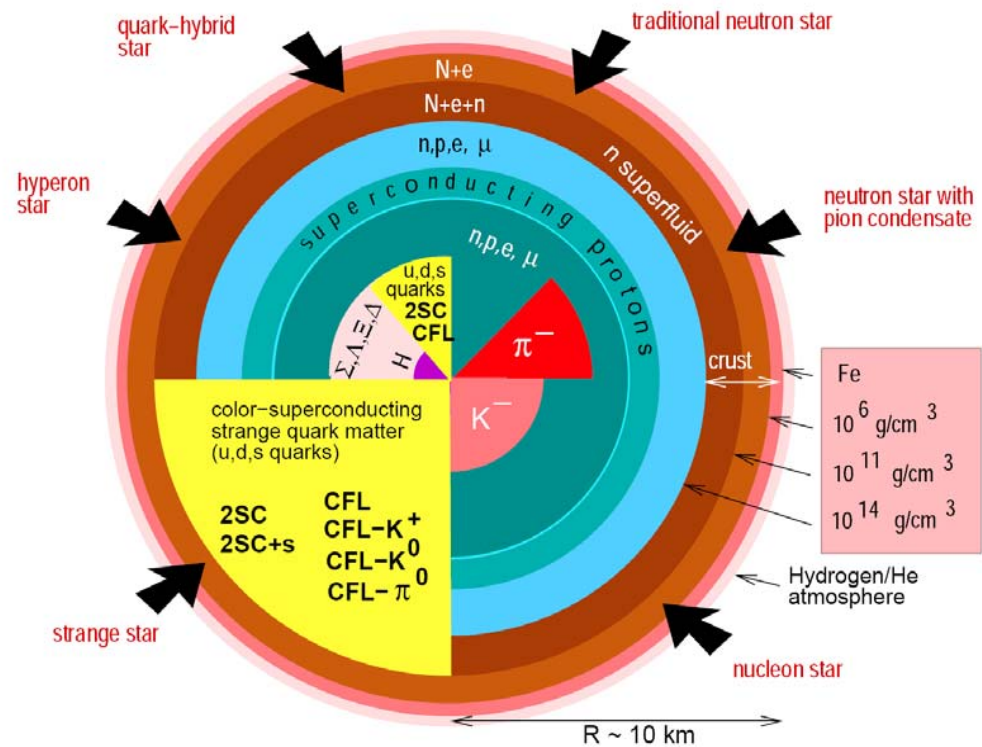CFL−π⁰

strange star

nucleon star

$R \sim 10$ km

Fig. 1. Competing structures and novel phases of subatomic matter predicted by theory to make their appearances in the cores ($R \lesssim 8$ km) of neutron stars[4].

significant range of chemical potentials and strange quark masses[51]. If the strange quark mass is heavy enough to be ignored, then up and down quarks may pair in the two-flavor superconducting (2SC) phase. Other possible condensation patters

color−superconducting strange quark matter (u,d,s quarks)

K. Rajagopal and F. Wilczek, *The Condensed Matter Physics of QCD*, At the Frontier of Particle Physics / Handbook of QCD, ed. M. Shifman, (World Scientific) (2001). M. Alford, Ann. Rev. Nucl. Part. Sci. **51** (2001) 131.

How we can detect a nuclear matter with the high density?

The quantum theory saying: we need to study the processes with extremely large transfer momentum

What we can see in processes with different probes ?

Electromagnetic probes
Hadrons and nuclei probes

DIS with leptons

Region 5

the region $x > 1$ the struck quark is 'superfast', its momentum is larger than momentum allowed for a stationary nucleon. The longitudinal distances involved < 0.2 fm and therefore one is sensitive to correlations of nearby nucleons or more cated configurations like multiquark clusters. As an example the predictions for iquark cluster calculation [32] are shown in figure 5.
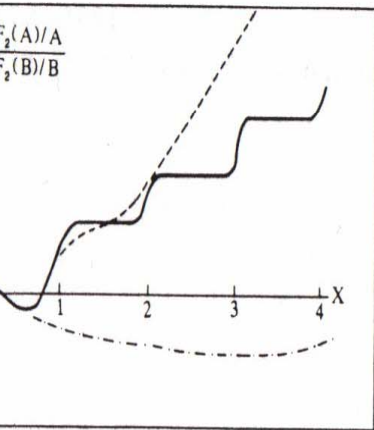
The height of the plateau in the range $1 < x < 2$ is proportional to the ra probabilities of finding 6-quark clusters in nuclei A and B, the range $2 < x < 3$ re the ratio of 9-quark cluster probabilities and so on.

Figure 6 shows preliminary results for the cross section ratio of Fe and He ob by NE-2 at SLAC [33], which took data for a series of nuclei with beam energies be 4 and 14 GeV. One could speculate that the plateau for $1.5 < x < 2$ is an indi for the step function expected in the multiquark cluster model. Note, however, th data are still substantially affected by quasielastic scattering as the ratio is smaller one near $x = 1$.

32 J. Vary, Proceedings of the 7th Int. Conf. on High Energy Physics p Dubna 1984,147.

5. Theoretical predictions for structure functions at $x > 1$
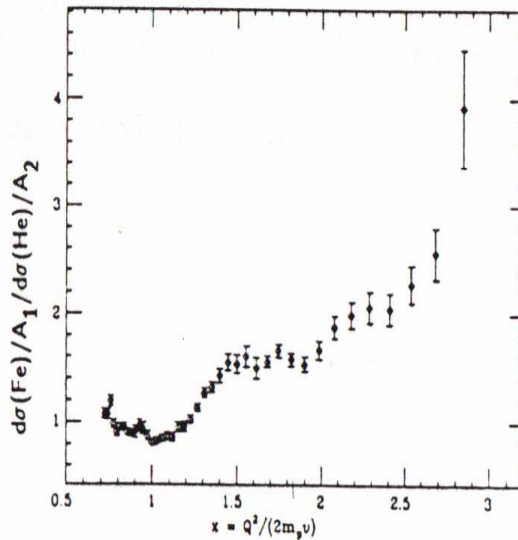
Figure 6. Preliminary results for σ^{Fe}/σ^{He} from NE-2 at SLAC

Nuclear structure functions in carbon near $x = 1$

BCDMS Collaboration

A.C. Benvenuti, D. Bollini, T. Camporesi[1], L. Monari[*], F.L. Navarria
Dipartimento di Fisica dell'Università and INFN, Bologna, Italy

A. Argento[2], J. Cvach[3], W. Lohmann[4], L. Piemontese[5]
CERN, Geneva, Switzerland

V.I. Genchev[6], J. Hladky[3], I.A. Golutvin, Yu.T. Kiryushin, V.S. Kiselev, V.G. Krivokhizhin, V.V. Kukhtin,
S. Nemeček[3], D.V. Peshekhonov, P. Reimer[3], I.A. Savin, G.I. Smirnov, S. Sultanov[6], A.G. Volodko and J. Začek[7]
Joint Institut for Nuclear Research, Dubna, Russia

D. Jamnik[8], R. Kopp[9], U. Meyer-Berkhout, A. Staude, K.-M. Teichert, R. Tirler[10], R. Voss[1], Č. Zupančič
Sektion Physik der Universität, München, Germany[11]

J. Feltesse, A. Misztajn, A. Ouraou, P. Rich-Hennion, Y. Sacquin, G. Smadja, P. Verrecchia, M. Virchaux
DAPNIA-SPP, Centre d'Etudes de Saclay, CEA, Gif-sur-Yvette, France

Abstract. Data from deep inelastic scattering of $200\,\mathrm{GeV}$ muons on a carbon target with squared four-momentum transfer $52\,\mathrm{GeV}^2 \leq Q^2 \leq 200\ \mathrm{GeV}^2$ were analysed in the region of the Bjorken variable close to $x = 1$, which is the kinematic limit for scattering on a free nucleon. At this value of x, the carbon structure function is found to be $F_2^C \approx 1.2 \cdot 10^{-4}$. The x dependence of the structure function for $x > 0.8$ is well described by an exponential $F_2^C \propto \exp(-sx)$ with $s = 16.5 \pm 0.6$.
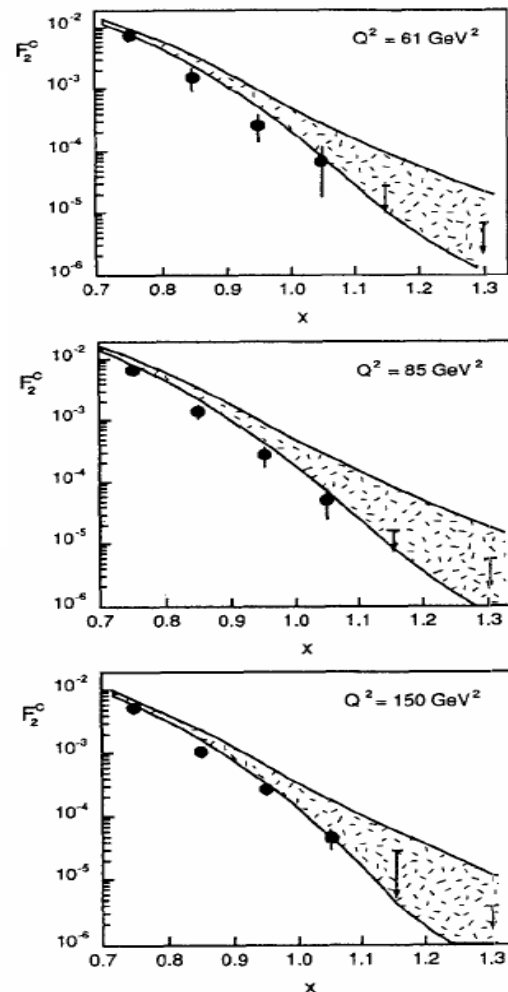
Fig. 7. The nuclear structure function $F_2^C(x)$ as a function of x, at three different values of Q^2. The hatched regions show the range of predictions of [26]

JLAB data

Observation of nuclear scaling in the $A(e,e')$ reaction at $x_B > 1$

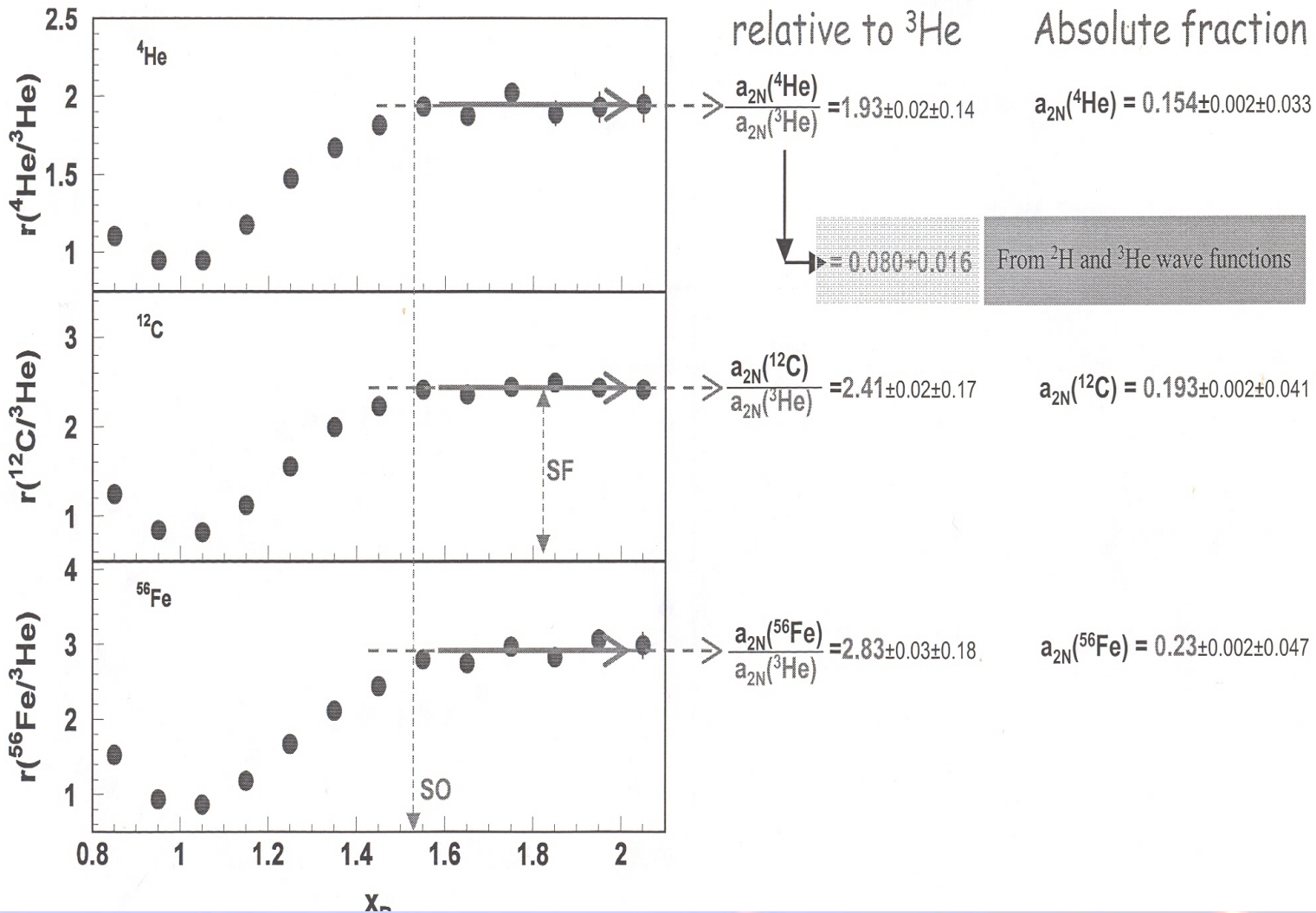## Measurement of Two- and Three-Nucleon Short-Range Correlation Probabilities in Nuclei

K. S. Egiyan,[1,34] N. B. Dashyan,[1] M. M. Sargsian,[10] M. I. Strikman,[28] L. B. Weinstein,[27] G. Adams,[30] P. Ambrozewicz,[10] M. Anghinolfi,[16] B. Asavapibhop,[22] G. Asryan,[1] H. Avakian,[34] H. Baghdasaryan,[27] N. Baillie,[38] J. P. Ball,[2] N. A. Baltzell,[33] V. Batourine,[20] M. Battaglieri,[16] I. Bedlinskiy,[18] M. Bektasoglu,[27] M. Bellis,[30,4] N. Benmouna,[12] A. S. Biselli,[30,4] B. E. Bonner,[31] S. Bouchigny,[34,17] S. Boiarinov,[34] R. Bradford,[4] D. Branford,[9] W. K. Brooks,[34] S. Bültmann,[27] V. D. Burkert,[34] C. Bulteceanu,[38] J. R. Calarco,[24] S. L. Careccia,[27] D. S. Carman,[26] B. Carnahan,[5] S. Chen,[11] P. L. Cole,[34,14] P. Coltharp,[11,34] P. Corvisiero,[16] D. Crabb,[37] H. Crannell,[5] J. P. Cummings,[30] E. De Sanctis,[15] R. DeVita,[16] P. V. Degtyarenko,[34] H. Denizli,[29] L. Dennis,[11] K. V. Dharmawardane,[27] C. Djalali,[33] G. E. Dodge,[27] J. Donnelly,[13] D. Doughty,[7,34] P. Dragovitsch,[11] M. Dugger,[2] S. Dytman,[29] O. P. Dzyubak,[33] H. Egiyan,[24] L. Elouadrhiri,[34] A. Empl,[30] P. Eugenio,[11] R. Fatemi,[37] G. Fedotov,[23] R. J. Feuerbach,[4] T. A. Forest,[27] H. Funsten,[38] G. Gavalian,[27] N. G. Gevorgyan,[1] G. P. Gilfoyle,[32] K. L. Giovanetti,[19] F. X. Girod,[6] J. T. Goetz,[3] E. Golovatch,[16] R. W. Gothe,[33] K. A. Griffioen,[38] M. Guidal,[17] M. Guillo,[33] N. Guler,[27] L. Guo,[34] V. Gyurjyan,[34] C. Hadjidakis,[17] J. Hardie,[7,34] F. W. Hersman,[24] K. Hicks,[26] I. Hleiqawi,[26] M. Holtrop,[24] J. Hu,[30] M. Huertas,[33] C. E. Hyde-Wright,[27] Y. Ilieva,[12] D. G. Ireland,[13] B. S. Ishkhanov,[23] M. M. Ito,[34] D. Jenkins,[36] H. S. Jo,[17] K. Joo,[37,8] H. G. Juengst,[12] J. D. Kellie,[13] M. Khandaker,[25] K. Y. Kim,[29] K. Kim,[20] W. Kim,[27,20] A. Klein,[27,20] F. J. Klein,[27] A. Klimenko,[27] M. Klusman,[30] L. H. Kramer,[10,34] V. Kubarovsky,[30] J. Kuhn,[4] S. E. Kuhn,[27] S. Kuleshov,[18] J. Lachniet,[4] J. M. Laget,[6,34] J. Langheinrich,[33] D. Lawrence,[22] T. Lee,[24] K. Livingston,[13] L. C. Maximon,[12] S. McAleer,[11] B. McKinnon,[13] J. W. C. McNabb,[4] B. A. Mecking,[34] M. D. Mestayer,[34] C. A. Meyer,[4] T. Mibe,[26] K. Mikhailov,[18] R. Minehart,[37] M. Mirazita,[15] R. Miskimen,[22] V. Mokeev,[23,34] S. A. Morrow,[6,17] J. Mueller,[29] G. S. Mutchler,[31] P. Nadel-Turonski,[12] J. Napolitano,[30] R. Nasseripour,[10] S. Niccolai,[12,17] G. Niculescu,[26,19] I. Niculescu,[12,19] B. B. Niczyporuk,[34] R. A. Niyazov,[34] G. V. O'Rielly,[22] M. Osipenko,[16,23] A. I. Ostrovidov,[11] K. Park,[20] E. Pasyuk,[2] C. Peterson,[13] J. Pierce,[37] N. Pivnyuk,[18] D. Pocanic,[37] O. Pogorelko,[18] E. Polli,[15] S. Pozdniakov,[18] B. M. Preedom,[33] J. W. Price,[3] Y. Prok,[34] D. Protopopescu,[13] L. M. Qin,[27] B. A. Raue,[10,34] G. Riccardi,[11] G. Ricco,[16] M. Ripani,[16] B. G. Ritchie,[2] F. Ronchetti,[15] G. Rosner,[13] P. Rossi,[15] D. Rowntree,[21] P. D. Rubin,[32] F. Sabatié,[27,6] C. Salgado,[25] J. P. Santoro,[36,34] V. Sapunenko,[16,34] R. A. Schumacher,[4] V. S. Serov,[18] Y. G. Sharabian,[34] J. Shaw,[22] E. S. Smith,[34] L. C. Smith,[37] D. I. Sober,[5] A. Stavinsky,[18] S. Stepanyan,[34] B. E. Stokes,[11] P. Stoler,[30] S. Strauch,[33] R. Suleiman,[21] M. Taiuti,[16] S. Taylor,[31] D. J. Tedeschi,[33] R. Thompson,[29] A. Tkabladze,[27,26] S. Tkachenko,[27,26] L. Todor,[4] C. Tur,[33] M. Ungaro,[30,8] M. F. Vineyard,[35,32] A. V. Vlassov,[18] D. P. Weygand,[34] M. Williams,[4] E. Wolin,[34] M. H. Wood,[33] A. Yegneswaran,[34] J. Yun,[27] L. Zana,[24] and J. Zhang[27]

(CLAS Collaboration)

2 nucleon correlations

relative to ^{3}He

$\dfrac{a_{2N}(^4He)}{a_{2N}(^3He)} = 1.93 \pm 0.02 \pm 0.14$

$= 0.080 + 0.016$ From ^{2}H and ^{3}He wave functions

$\dfrac{a_{2N}(^{12}C)}{a_{2N}(^3He)} = 2.41 \pm 0.02 \pm 0.17$

$\dfrac{a_{2N}(^{56}Fe)}{a_{2N}(^3He)} = 2.83 \pm 0.03 \pm 0.18$

Absolute fraction

$a_{2N}(^4He) = 0.154 \pm 0.002 \pm 0.033$

$a_{2N}(^{12}C) = 0.193 \pm 0.002 \pm 0.041$

$a_{2N}(^{56}Fe) = 0.23 \pm 0.002 \pm 0.047$

3 nucleon correlations

relative to ^{3}He   Absolute fraction

$\dfrac{a_{3N}(^4He)}{a_{3N}(^3He)} = 2.33 \pm 0.12 \pm 0.19$ $a_{3N}(^4He) = 0.42 \pm 0.02 \pm 0.14$

$= 0.0018 \pm 0.0006$ (M. Sargsyan's calculations)

$\dfrac{a_{3N}(^{12}C)}{a_{3N}(^3He)} = 3.05 \pm 0.14 \pm 0.22$ $a_{3N}(^{12}C) = 0.55 \pm 0.03 \pm 0.18$

$\dfrac{a_{3N}(^{56}Fe)}{a_{3N}(^3He)} = 4.38 \pm 0.18 \pm 0.33$ $a_{3N}(^{56}Fe) = 0.79 \pm 0.03 \pm 0.25$

Having these data, we know almost full (≈99%) nucleonic picture of nuclei with A ≤ 56

Fractions / Nucleus	Single particle (%)	2N SRC (%)	3N SRC (%)
^{56}Fe	**76** ± 0.2 ± 4.7	**23.0** ± 0.2 ± 4.7	**0.79** ± 0.03 ± 0.25
^{12}C	**80** ± 02 ± 4.1	**19.3** ± 0.2 ± 4.1	**0.55** ± 0.03 ± 0.18
^{4}He	**86** ± 0.2 ± 3.3	**15.4** ± 0.2 ± 3.3	**0.42** ± 0.02 ± 0.14
^{3}He	**92** ± 1.6	**8.0** ± 1.6	**0.18** ± 0.06
^{2}H	**96** ± 0.8	**4.0** ± 0.8	-----

Using the published data on (p,2p+n) [PRL,90 (2003) 042301] estimate the isotopic composition of 2N SRC in ^{12}C

$a_{2N}(^{12}C) \approx 20 \pm 0.2 \pm 4.1$ % ⟶

$a_{pp}(^{12}C) \approx 4 \pm 2$ %
$a_{pn}(^{12}C) \approx 12 \pm 4$ %
$a_{nn}(^{12}C) \approx 4 \pm 2$ %

Asymptotic form factors of hadrons and nuclei and the continuity of particle and nuclear dynamics

Stanley J. Brodsky*

Stanford Linear Accelerator Center, Stanford University, Stanford, California 94305

Benson T. Chertok†

American University, Washington, D. C. 20016

(Received 7 June 1976)

The large-q^2 behavior of the elastic form factor of a hadron or nucleus is related by dimensional counting to the number of its elementary constituents. Using the framework of a scale-invariant quark model, dimensional-scaling predictions are derived for the $B(q^2)/A(q^2)$ ratio in the Rosenbluth formula, multiple-photon-exchange corrections, and the mass parameters which control the onset of the asymptotic power law in the meson, nucleon, and deuteron form factors. A simple "democratic chain" model predicts that for large q^2, $F(q^2) \propto (1 - q^2/m_n{}^2)^{1-n}$, where $m_n{}^2$ is proportional to the number of constituents n. In the case of nuclear targets (or systems with several scales of compositeness), we also define the "reduced" form factor $f_A(q^2) = F_A(q^2)/\Pi_{i=1}^{A} F_i(q_i{}^2)$ in order to remove the minimal falloff of F_A due to the nucleon form factors at $q_i{}^2 = (m_i{}^2/M_A{}^2)q^2$. Dimensional counting predicts $(q^2)^{A-1}f_A(q^2) \to$ const. A systematic comparison of the data for π, p, n, and deuteron form factors with the dimensional-scaling quark-model predictions is given. Predictions are made for the large-spacelike-q^2 ^{3}He and α-particle form factors. We also relate the deuteron form factor to (off-shell) fixed-angle n-p scattering, and show that the experimental results for $t^5 F_d(t)$ are consistent with the magnitude of the s-wave wave function $u'(0)$ obtained from soft-core potentials. The relation of the dynamics of an underlying six-quark state of the deuteron to the nucleon-potential and meson-exchange-current contributions is discussed. The scaling of $q^2 f_d(q^2)$ implies that the nuclear potential (after removing the effects of nucleon structure) displays the scale-invariant behavior of a theory without a fundamental length scale. Predictions are also given for the structure functions, fragmentation, and large-angle scattering of a nucleus.
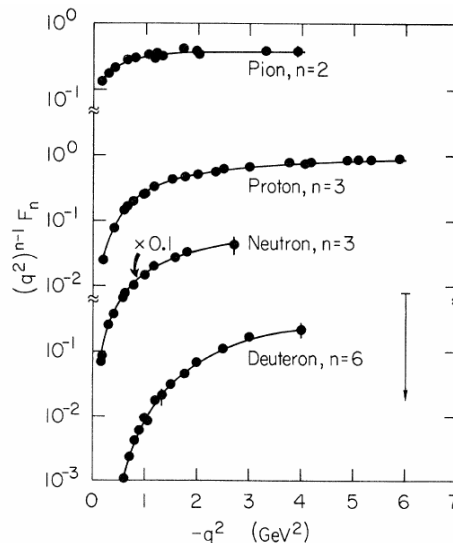
FIG. 1. Elastic electromagnetic form factors of hadrons for large spacelike q^2 in terms of the dimensional-scaling quark model. The curves simply connect the data points. (The neutron data have been multiplied by 0.1.)

Hadrons and nuclei probes

1. High p_T processes

2. Cumulative and subthreshold processes

A.V.Efremov, V.T.Kim, G.I.Lykasov

HARD HADRON-NUCLEUS PROCESSES AND MULTIQUARK CONFIGURATIONS IN NUCLEI

V. Conclusion

The analysis of the inclusive large $x_\perp$ meson production in the hard hadron processes on nuclei has allowed one to understand the relative contribution of multiple rescattering processes and the existence of multiquark fluctons in the nucleus in dependence on $x_\perp$ the multiple rescattering processes are dominating at $x_\perp < 0.7 \div 0.8$ whereas at larger $x_\perp$ the mechanism of hard scattering on fluctons is dominating. The model of multiple rescattering in which the multiple soft collisions suggested in this paper are taken into account before the hard collision allows one to describe the multiple rescattering processes inside the nucleus correctly.

The flucton model successfully used earlier for the description of the cumulative production and EMC-effect with such parameters is applied for the description of anomalous phenomena in the large $p_\perp$ processes in nuclei.

In 1973 were published two artiles :

Matveev V.A., Muradyan R.M., Tavkhelidze A.N. Lett. Nuovo Cimento 7,719 (1973);

Brodsky S., Farrar G. Phys. Rev. Lett. 31,1153 (1973)

Predictions that for momentum $p_{beam} \geq 5$ GeV/c in any binary large-angle scattering ($\theta_{cm} > 40°$) reaction at large momentum transfers $Q = \sqrt{-t}$:

$$A + B \rightarrow C + D$$

$$\frac{d\sigma}{dt}_{A+B \rightarrow C+D} \sim s^{-(n_A+n_B+n_C+n_D-2)} f(\frac{t}{s})$$

where n_A, n_B, n_C and n_D the amounts of elementary constituents in A,B,C and D.

$$s=(p_A+p_B)^2 \quad \text{and} \quad t=(p_A-p_C)^2,$$

$$\frac{d\sigma}{dt}_{pp \rightarrow pp} \sim s^{-10} \quad \text{and} \quad \frac{d\sigma}{dt}_{\pi p \rightarrow \pi p} \sim s^{-8}$$

Scaling Laws at Large Transverse Momentum*

Stanley J. Brodsky
Stanford Linear Accelerator Center, Stanford University, Stanford, California 94305

and

Glennys R. Farrar
California Institute of Technology, Pasadena, California 91109
(Received 14 August 1973)

The application of simple dimensional counting to bound states of pointlike particles enables us to derive scaling laws for the asymptotic energy dependence of electromagnetic and hadronic scattering at fixed c.m. angle which only depend on the number of constituent fields of the hadrons. Assuming quark constituents, some of the $s \to \infty$, fixed-t/s predictions are $(d\sigma/dt)_{\pi p \to \pi p} \sim s^{-8}$, $(d\sigma/dt)_{pp \to pp} \sim s^{-10}$, $(d\sigma/dt)_{\gamma p \to \pi p} \sim s^{-7}$, $(d\sigma/dt)_{\gamma p \to \gamma p} \sim s^{-6}$, $F_\pi(q^2) \sim (q^2)^{-1}$, and $F_{1p}(q^2) \sim (q^2)^{-2}$. We show that such scaling laws are characteristic of renormalizable field theories satisfying certain conditions.

Our central result for exclusive scattering[1] is

$$(d\sigma/dt)_{AB \to CD} \sim s^{2-n} f(t/s) \qquad (1)$$

($s \to \infty$, t/s fixed). Here n is the total number of leptons, photons, and quark components (i.e., elementary fields) of the initial and final states. This result follows heuristically if the only physical dimensional quantities are particle masses and momenta. We begin by considering a world in which a hadron would become a collection of free quarks with equal momenta if the strong interactions were turned off. Note that the dimen-

[1]This result for elastic scattering has been obtained independently by V. Matveev, R. Muradyan, and A. Tavkhelidze, Joint Institute for Nuclear Research Report No. D2-7110, 1973 (to be published). We thank J. Kiskis for bringing this work to our attention.
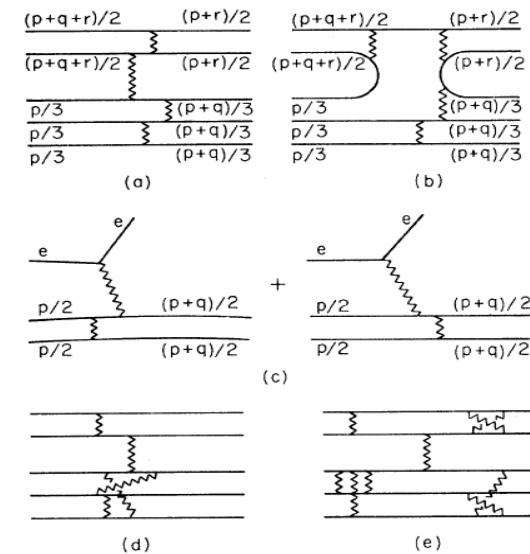
FIG. 1. Typical Born diagrams for large-momentum-transfer elastic scattering in the quark picture. (a) $\pi p \to \pi p$ (quark scattering), (b) $\pi p \to \pi p$ (quark interchange), (c) $e\pi \to e\pi$, (d) an irreducible loop diagram, (e) a reducible loop diagram.

Unified description of inclusive and exclusive reactions at all momentum transfers*

R. Blankenbecler and S. J. Brodsky

$$E \frac{d\sigma}{d^3p} (A + B \rightarrow C + X) \rightarrow (p_T^2)^{-N} f\left(\frac{\mathfrak{M}^2}{s}, \frac{t}{s}\right)$$

and[5,6]

$$\frac{d\sigma}{dt} (A + B \rightarrow C + D) \rightarrow (p_T^2)^{-N} f\left(\frac{t}{s}\right)$$

The entire kinematic range of high-energy inclusive reactions is illustrated on the Peyrou plot of Fig. 1. As usual we define

$$s = (p_A + p_B)^2, \quad t = (p_A - p_C)^2,$$

$$u = (p_B - p_C)^2, \quad \mathfrak{M}^2 = (p_A + p_B - p_C)^2,$$

and

$$\epsilon = \mathfrak{M}^2/s \cong (1 - p_{c.m.}/p_{max}),$$

$$x_T = p_T/p_{max}, \quad x_L = p_L/p_{max} \simeq (t - u)/s.$$

TABLE I. The expected dominant subprocesses for selected hadronic inclusive reactions at large transverse momentum. The second column lists the important exclusive processes which contribute to each inclusive cross section at $\epsilon \sim 0$. The basic subprocesses expected in the CIM, and the resulting form of the inclusive cross section $E d\sigma/d^3p \sim (p_\perp^2)^{-N} \epsilon^P$ for $p_\perp^2 \sim \infty$, $\epsilon \rightarrow 0$, and fixed $\theta_{c.m.}$ are given in the last columns. The subprocesses that have the dominant $p_\perp$ dependence at fixed ϵ are underlined. For some particular final-state quantum numbers, the above powers of ϵ should be increased.

Inclusive process	Exclusive-limit channel	Subprocesses	$\frac{d\sigma}{d^3p/E}$ $(\theta \sim 90°)$
$M + B \rightarrow M + X$	$M + B \rightarrow M + B*$ $(n = 10)$	$\underline{M + q \rightarrow M + q}$	$(p_\perp^2)^{-4} \epsilon^3$
		$\bar{q} + B \rightarrow M + qq$	$(p_\perp^2)^{-6} \epsilon^1$
		$M + B \rightarrow M + B*$	$(p_\perp^2)^{-8} \epsilon^{-1}$
$B + B \rightarrow B + X$	$B + B \rightarrow B + B*$ $(n = 12)$	$\underline{B + q \rightarrow B + q}$	$(p_\perp^2)^{-6} \epsilon^3$
		$\underline{(qq) + (qq) \rightarrow B + q}$	$(p_\perp^2)^{-6} \epsilon^3$
		$B + (qq) \rightarrow B + qq$	$(p_\perp^2)^{-8} \epsilon^1$
		$B + B \rightarrow B + B*$	$(p_\perp^2)^{-10} \epsilon^{-1}$
	$B + B \rightarrow B + B* + M*$ $(n = 14)$	$\underline{q + q \rightarrow B + \bar{q}}$	$(p_\perp^2)^{-4} \epsilon^7$
		$q + (qq) \rightarrow B + M*$	$(p_\perp^2)^{-6} \epsilon^5$
		$(qq) + B \rightarrow B + M* + qq$	$(p_\perp^2)^{-10} \epsilon^1$
		$B + B \rightarrow B + B* + M*$	$(p_\perp^2)^{-12} \epsilon^{-1}$
$B + B \rightarrow M + X$	$B + B \rightarrow M + B* + B*$ $(n = 14)$	$\underline{q + (qq) \rightarrow M + B*}$	$(p_\perp^2)^{-6} \epsilon^5$
		$q + B \rightarrow q(\rightarrow M + q) + B*$	$(p_\perp^2)^{-6} \epsilon^5$
		$q + B \rightarrow M + q + B*$	$(p_\perp^2)^{-8} \epsilon^3$
		$(qq) + B \rightarrow M + B* + qq$	$(p_\perp^2)^{-10} \epsilon^1$
		$B + B \rightarrow M + B* + B*$	$(p_\perp^2)^{-12} \epsilon^{-1}$
	$B + B \rightarrow M + M* + B* + B*$ $(n = 16)$	$\underline{M + q \rightarrow M + q}$	$(p_\perp^2)^{-4} \epsilon^9$
		$q + q \rightarrow \bar{q}(\rightarrow M + \bar{q}) + B*$	$(p_\perp^2)^{-4} \epsilon^9$
		$q + q \rightarrow M + B* + \bar{q}$	$(p_\perp^2)^{-6} \epsilon^7$
		$M + B \rightarrow M + B*$	$(p_\perp^2)^{-8} \epsilon^5$
	$B + B \rightarrow M + M* + M* + B* + B*$ $(n = 18)$	$\underline{q + \bar{q} \rightarrow M + M*}$	$(p_\perp^2)^{-4} \epsilon^{11}$
		$\underline{q + M \rightarrow q(\rightarrow M + q) + M*}$	$(p_\perp^2)^{-4} \epsilon^{11}$
$B + B \rightarrow \bar{B} + X$	$B + B \rightarrow \bar{B} + B* + B* + \bar{B}*$ $(n = 18)$	$\underline{q + q \rightarrow B* + \bar{q}(\rightarrow \bar{B} + qq)}$	$(p_\perp^2)^{-4} \epsilon^{11}$
		$q + q \rightarrow B* + \bar{B} + qq$	$(p_\perp^2)^{-8} \epsilon^7$
		$q + (qq) \rightarrow \bar{B} + B* + B*$	$(p_\perp^2)^{-10} \epsilon^5$

S.J. Brodsky, J.F.Gunion

RECENT DEVELOPMENTS IN THE THEORY OF LARGE TRANSVERSE MOMENTUM PROCESSES*

TABLE I

Scaling Predictions for $E\, d\sigma/d^3p = C\, p_T^{-n}(1-x_T)^F$

Large p_T Process	Leading CIM Subprocess	Predicted	Observed (CP)$^\varepsilon$
		n//F	n//F
$pp \to \pi^+ X$	$qM \to q\pi^+$	8//9	8.5//8.8
π^-	$qM \to q\pi^-$	8//9	8.9//9.7
K^+	$qM \to qK^+$	8//9	8.4//8.8
K^-	$qM \to qK^-$	8//13	8.9//11.7
	$q\bar{q} \to K^+K^-$	8//11	
$pp \to pX$	$q(qq) \to Mp$	12//5	11.7//6.8
	$qB \to qp$	12//7	
$pp \to \bar{p}X$	$q\bar{q} \to B\bar{p}$	12//11	8.8//14.2
	$qM \to qM$	8//15	
$\pi p \to \pi X$	$q\bar{q} \to M\pi$	8//5	
	$qM \to q\pi$	8//7	
	$q(qq) \to B\pi$	12//3	
	$\pi q \to \pi q$	8//3	

Indication of asymptotic scaling in the reactions $dd \to p^3H$, $dd \to n^3He$ and $pd \to pd$

Yu. N. Uzikov[1]

Joint Institute for Nuclear Research, LNP, 141980 Dubna, Moscow region, Russia

Submitted 11 January 2005
Resubmitted 28 February 2005

It is shown that the differential cross sections of the reactions $dd \to n^3He$ and $dd \to p^3H$ measured at c.m.s. scattering angle $\theta_{cm} = 60°$ in the interval of the deuteron beam energy 0.5–1.2 GeV demonstrate the scaling behaviour, $d\sigma/dt \sim s^{-22}$, which follows from constituent quark counting rules. It is found also that the differential cross section of the elastic $dp \to dp$ scattering at $\theta_{cm} = 125-135°$ follows the scaling regime $\sim s^{-16}$ at beam energies 0.5–5 GeV. These data are parameterized here using the Reggeon exchange.
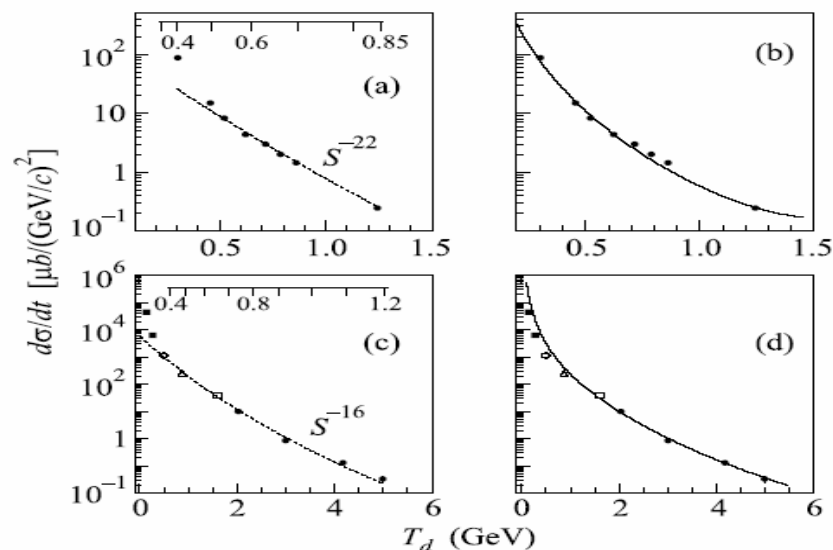
Fig.2. The differential cross section of the $dd \to n^3He$ and $dd \to p^3H$ reactions at $\theta_{cm} = 60°$ (a), (b) and $dp \to dp$ at $\theta_{cm} = 127°$ (c), (d) versus the deuteron beam kinetic energy. Experimental data in (a), (b) are taken from [20]. In (c), (d), the experimental data (black squares), (○), (△), (open square) and (●) are taken from [22 – 26], respectively. The dashed curves give the s^{-22} (a) and s^{-16} (c) behaviour. The full curves show the result of calculations using Regge formalism given by Eqs. (2), (3), (4) with the following parameters: (b) – $C_1 = 1.9\,\text{GeV}^2$, $R_1^2 = 0.2\,\text{GeV}^{-2}$, $C_2 = 3.5$, $R_2^2 = -0.1\,\text{GeV}^{-2}$; (d) – $C_1 = 7.2\,\text{GeV}^2$, $R_1^2 = 0.5\,\text{GeV}^{-2}$, $C_2 = 1.8$, $R_2^2 = -0.1\,\text{GeV}^{-2}$. The upper scales in (a) and (c) show the relative momentum q_{pn} (GeV/c) in the deuteron for the ONE mechanism

pp (at 90o c.m.s.)
and cumulative
physics with polarized
beams.

ANTIPROTON ANNIHILATION IN QUANTUM CHROMODYNAMICS*

STANLEY J. BRODSKY
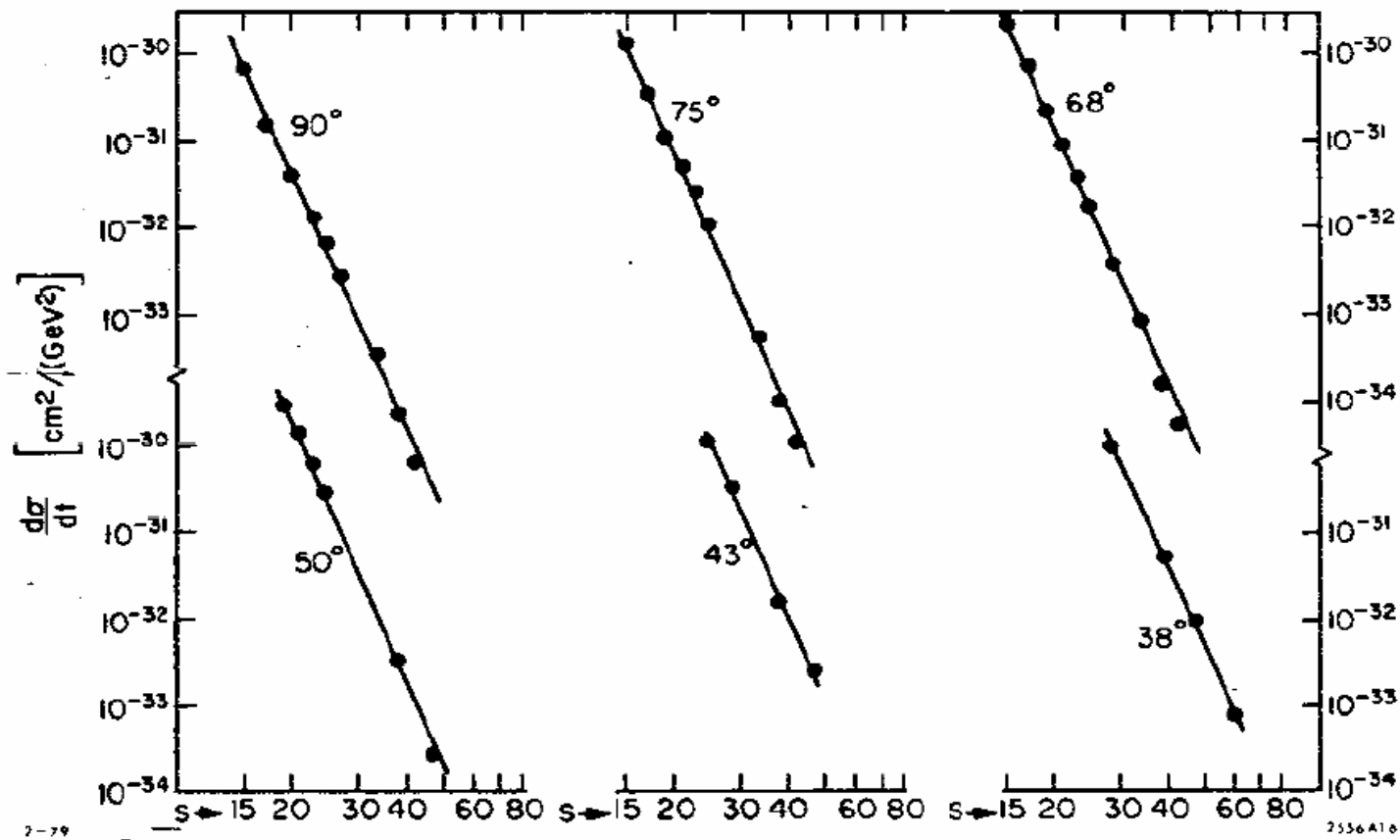
Fig. 16. Test of fixed θ_{CM} scaling for elastic pp scattering. The best fit gives the power $N = 9.7 \pm 0.5$ compared to the dimensional counting prediction $N=10$. Small deviations are not readily apparent on this log-log plot. The compilation is from Landshoff and Polkinghorne.

Elastic Proton-Proton Scattering at 90° and Structure within the Proton*

C. W. AKERLOF, R. H. HIEBER, A. D. KRISCH

Randall Laboratory of Physics, University of Michigan, Ann Arbor, Michigan

AND

K. W. EDWARDS†

Department of Physics, University of Iowa, Iowa City, Iowa

AND

L. G. RATNER

Particle Accelerator Division, Argonne National Laboratory, Argonne, Illinois

AND

K. RUDDICK‡

Department of Physics, University of Minnesota, Minneapolis, Minnesota

(Received 3 January 1964)

The differential cross section for proton-proton elastic scattering at 90° in the center-of-mass system was measured at laboratory momenta ranging from 5.0 to 13.4 GeV/c. Fifty-one measurements were made at momentum intervals of 100 or 200 MeV/c. The extracted proton beam of the ZGS impinged upon a CH_2 target. The two scattered protons were detected by two spectrometers consisting of magnets and scintillation counter telescopes in coincidence. The incident beam flux was measured by radiochemical analysis of the CH_2 targets. The experiment showed no evidence for any $S=0$, $T=1$ dibaryon resonances in the 3300–5200-MeV mass range. It also yielded some information about the validity of the statistical model and the analyticity of the scattering amplitude. The most interesting result of the experiment was a sharp break in the fixed-angle cross section. This may be evidence for the existence of two inner regions of the proton with radii $0.51\pm.02$ and $0.34\pm.02$ F.

TABLE I. Proton-proton elastic scattering cross sections at 90°
in the center-of-mass system.

$P_{c.m.}^2$ (GeV/c)^2	P_0 (GeV/c)	$(d\sigma/d\Omega)_{c.m.}$ (μb/sr)	$(d\sigma/dt)_{c.m.}$ μb/(GeV/c)^2	Error in $d\sigma/d\Omega$ & $d\sigma/dt$ %
1.946	5.0	8.51	13.74	2.9
1.993	5.1	7.90	12.45	3.3
2.039	5.2	7.09	10.93	3.1
2.086	5.3	6.49	9.77	3.6
2.132	5.4	5.53	8.15	3.1
2.178	5.5	4.90	7.07	3.4
2.223	5.6	4.47	6.32	3.1
2.270	5.7	3.72	5.15	3.3
2.316	5.8	3.37	4.57	3.3
2.363	5.9	2.74	3.64	3.5
2.409	6.0	2.44	3.18	3.1
2.456	6.1	2.19	2.80	3.7
2.503	6.2	1.83	2.30	3.7
2.595	6.4	1.50	1.82	3.7
2.686	6.6	1.07	1.25	4.7
2.779	6.8	0.796	0.900	4.7
2.873	7.0	0.645	0.706	4.1
2.965	7.2	0.515	0.546	4.0
3.059	7.4	0.386	0.396	4.8
3.151	7.6	0.305	0.304	5.4
3.247	7.8	0.253	0.245	4.5
3.338	8.0	0.217	0.204	4.5
3.386	8.1	0.169	0.157	3.9
3.434	8.2	0.172	0.157	4.4
3.480	8.3	0.154	0.139	3.8
3.527	8.4	0.153	0.136	4.6
3.618	8.6	0.127	0.110	4.6
3.713	8.8	0.103	0.0871	4.8
3.806	9.0	0.0809	0.0667	4.6
3.897	9.2	0.0780	0.0629	4.3
3.992	9.4	0.0676	0.0532	5.3
4.084	9.6	0.0589	0.0453	4.9
4.178	9.8	0.0536	0.0403	4.7
4.272	10.0	0.0468	0.0344	4.9
4.364	10.2	0.0441	0.0318	4.8
4.461	10.4	0.0386	0.0272	4.7
4.554	10.6	0.0356	0.0246	4.8
4.644	10.8	0.0303	0.0205	4.9
4.739	11.0	0.0284	0.0188	5.5
4.831	11.2	0.0255	0.0166	5.4
4.924	11.4	0.0202	0.0129	5.4
5.018	11.6	0.0190	0.0119	5.2
5.112	11.8	0.0153	0.00940	5.4
5.208	12.0	0.0143	0.00862	5.4
5.299	12.2	0.0118	0.00699	5.3
5.392	12.4	0.0116	0.00676	5.4
5.490	12.6	0.00953	0.00545	6.3
5.579	12.8	0.00867	0.00488	5.7
5.674	13.0	0.00739	0.00409	5.9
5.770	13.2	0.00722	0.00393	7.1
5.861	13.4	0.00525	0.00281	5.7

8 GeV/c
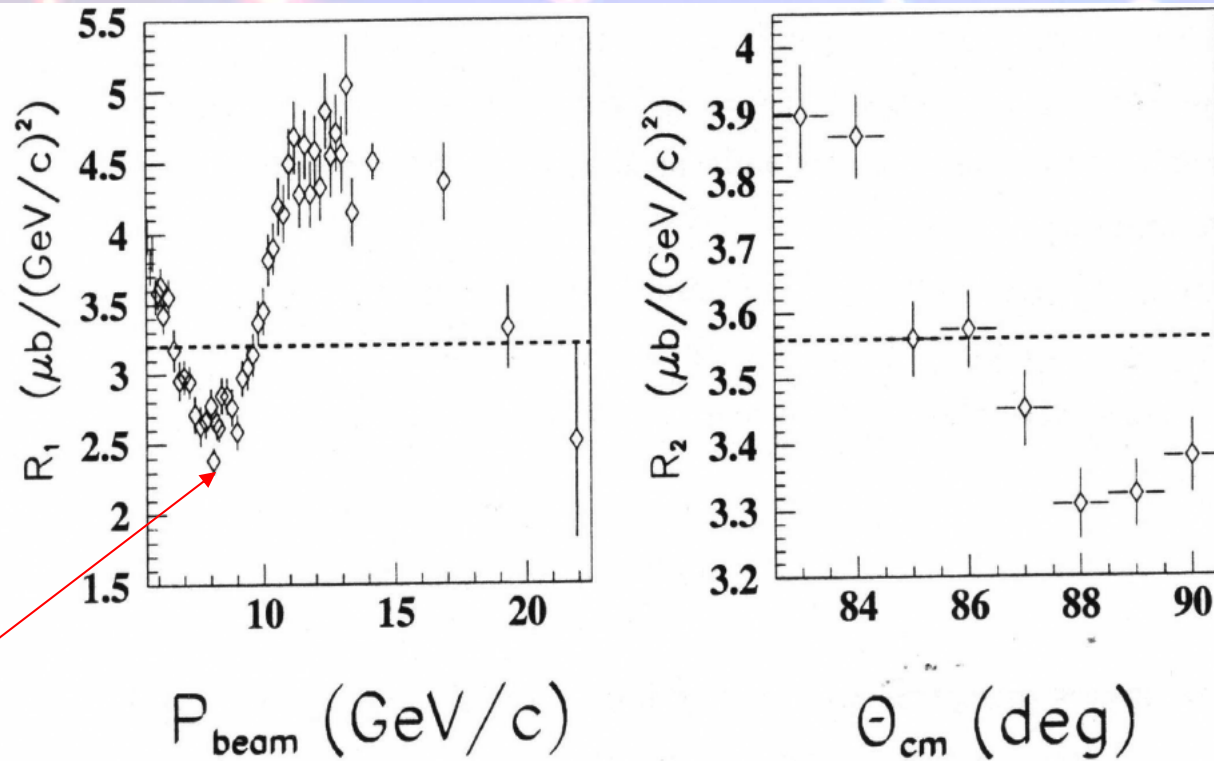
Figure 1.2: Scaled $pp \to pp$ differential cross sections. The dashed lines represent perfect scaling. Their vertical position is arbitrary. **Left** - $R_1 = \left(\left(\frac{s}{s_0}\right)^{10} \frac{d\sigma}{dt}(pp)\right)^{-1}$ $(s_0 = 13 \; GeV^2)$ at $\theta_{cm} = 90^0$ versus incoming momentum. Data are from Ref. [19]. **Right** - $R_2 = (1 - \cos^2 \theta_{cm})^{4\gamma} \frac{d\sigma}{dt}(pp)$ $(\gamma = 1.6)$ at $p_{lab} = 5.9$ GeV/c versus θ_{cm}. Data are from Ref. [17].

Energy dependence of spin-spin effects in p-p elastic scattering at $90°_{c.m.}$

E. A. Crosbie, L. G. Ratner, and P. F. Schultz
Argonne National Laboratory, Argonne, Illinois 60439

J. R. O'Fallon
Argonne Universities Association, Argonne, Illinois 60439

D. G. Crabb, R. C. Fernow,* P. H. Hansen,† A. D. Krisch, A. J. Salthouse,‡ B. Sandler,§ T. Shima, and
K. M. Terwilliger
Randall Laboratory of Physics, The University of Michigan, Ann Arbor, Michigan 48109

N. L. Karmakar
University of Kiel, Kiel, Germany

S. L. Linn‖ and A. Perlmutter
Department of Physics and Center for Theoretical Studies, The University of Miami, Coral Gables, Florida 33124

P. Kyberd
Nuclear Physics Laboratory, Oxford University, Oxford, England
(Received 31 March 1980)

The energy dependence of the spin-parallel and spin-antiparallel cross sections for $p_\uparrow + p_\uparrow \rightarrow p + p$ at $90°_{c.m.}$ was measured for beam momenta between 6 and 12.75 GeV/c. The ratio $(d\sigma/dt)_{parallel}$:$(d\sigma/dt)_{antiparallel}$ at 90° is about 1.2 up to 8 GeV/c and then increases rapidly to a value of almost 4 near 11 GeV/c. Our data indicate that this ratio may depend only on the variable $P_\perp^2$, and suggests that the ratio may reach a limiting value of about 4 for large $P_\perp^2$.
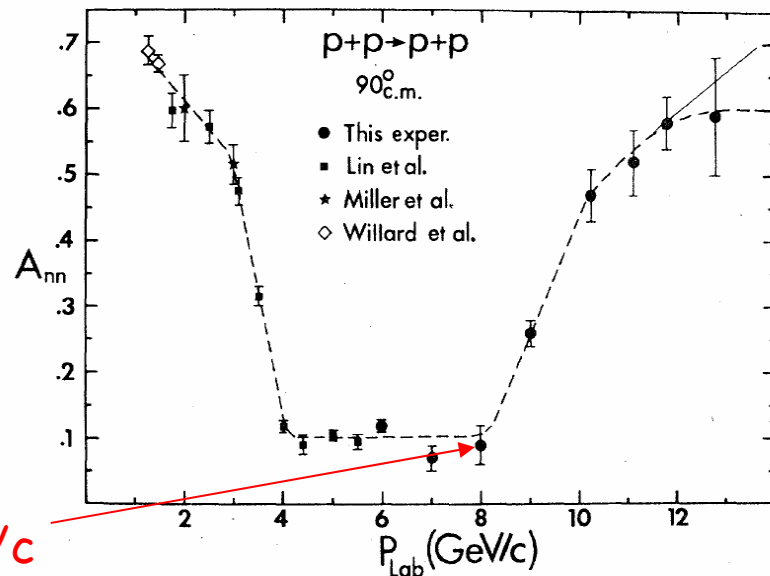
FIG. 2. Plot of the spin-spin correlation parameter A_{nn} for $p+p \rightarrow p+p$ at $90°_{c.m.}$ as a function of incident beam momentum. The dashed and solid lines are hand-drawn possible fits.
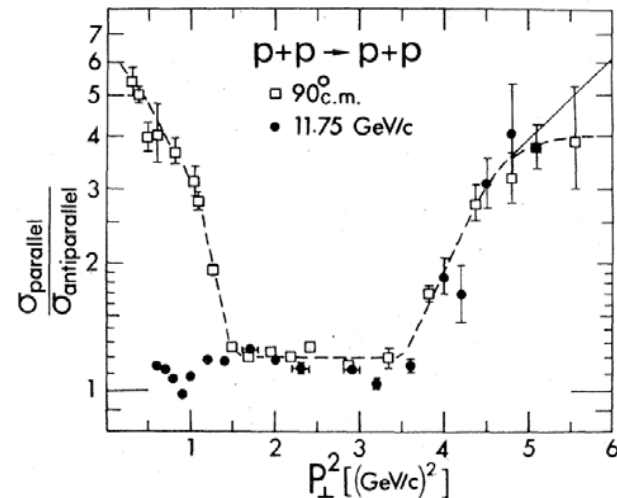
FIG. 3. Plot of the ratio of the spin-parallel to spin-antiparallel differential cross sections, as a function of $P_\perp^2$, for p-p elastic scattering. The squares are the fixed-angle data at $90°_{c.m.}$, with the incident energy varied. The circles are data (Refs. 5, 11) with the momentum held fixed at 11.75 GeV/c while the scattering angle is varied. The dashed and solid lines are hand-drawn possible fits to the $90°_{c.m.}$ data.

8 GeV/c

Color(nuclear) transparency in 90⁰ c.m. quasielastic $A(p,2p)$ reactions

The incident momenta varied from 5.9 to 14.4 GeV/c, corresponding to $4.8 < Q^2 < 12.7 (GeV/c)^2$.

$$T = \frac{\frac{d\sigma}{dt}(p + "p" \rightarrow p + p)}{Z\frac{d\sigma}{dt}(p + p \rightarrow p + p)}$$
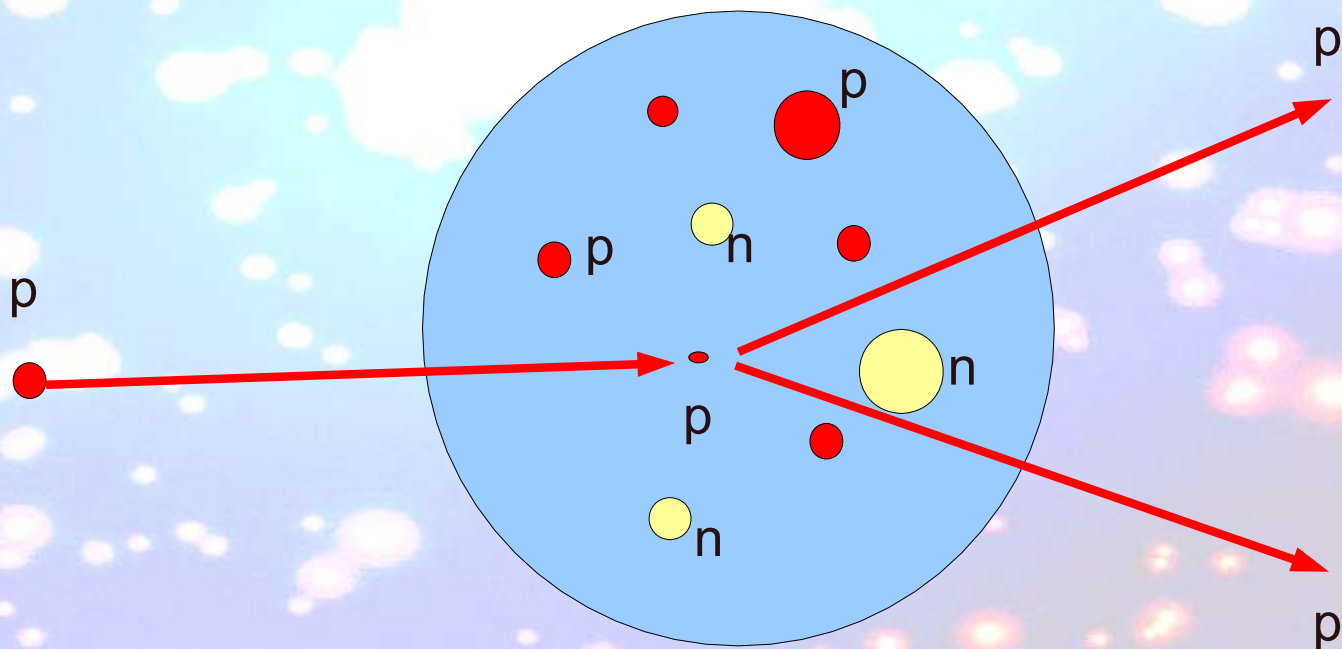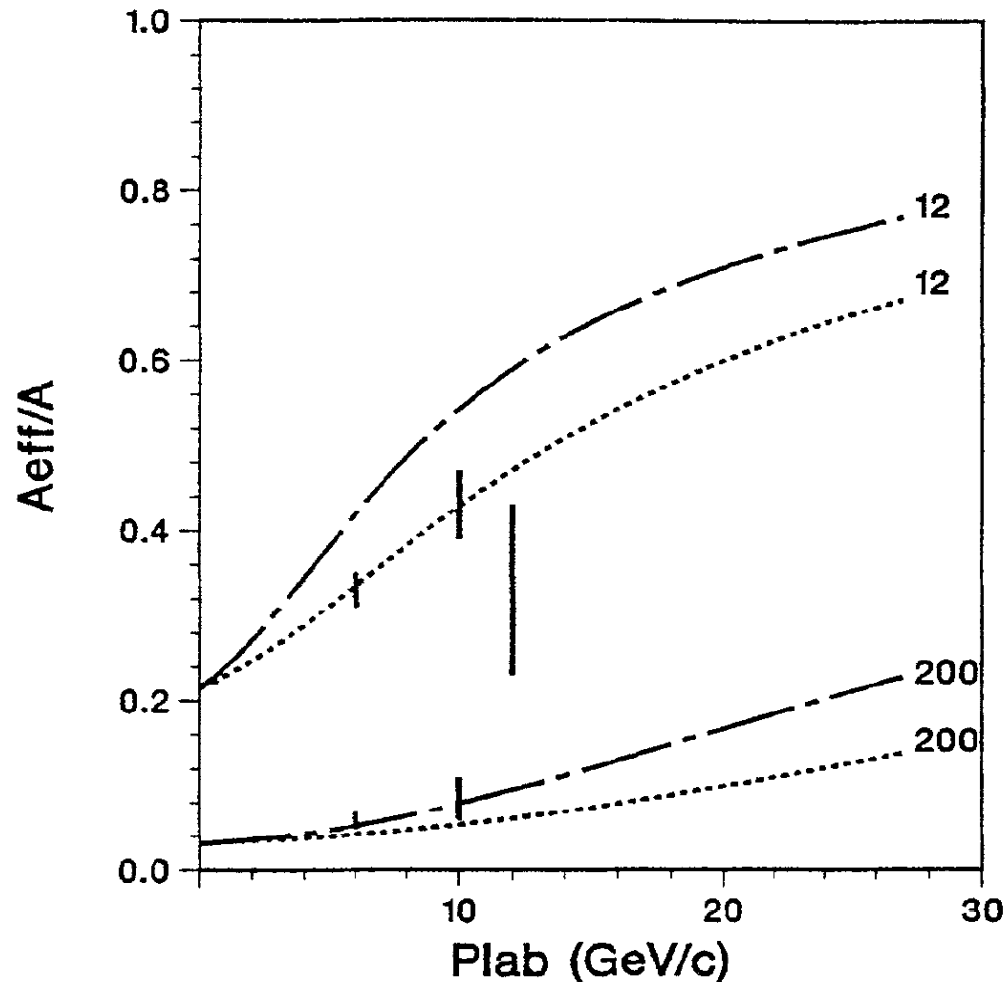
Fig. 3.8. The theoretical predictions of Farrar et al. [51] for $pA \to p'p''(A-1)$. The model predicts a monotonically increasing transparency ratio which is in clear conflict with the data, especially for the Al target (not shown; see Fig. 3.3).

A relativistic framework to determine the nuclear transparency from $A(p, 2p)$ reactions

B. Van Overmeire, J. Ryckebusch

Department of Subatomic and Radiation Physics, Ghent University,
Proeftuinstraat 86, B-9000 Gent, Belgium

tract

lativistic framework for computing the nuclear transparency extracted from
2p) scattering processes is presented. The model accounts for the initial- and
-state interactions (IFSI) within the relativistic multiple-scattering Glauber ap-
imation (RMSGA). For the description of color transparency, two existing mod-
re used. The nuclear filtering mechanism is implemented as a possible explana-
for the oscillatory energy dependence of the transparency. Results are presented
he target nuclei ^{7}Li, ^{12}C, ^{27}Al, and ^{63}Cu. An approximated, computationally
intensive version of the RMSGA framework is found to be sufficiently accurate
he calculation of the nuclear transparency. After including the nuclear filtering
color transparency mechanisms, our calculations are in acceptable agreement
the data.
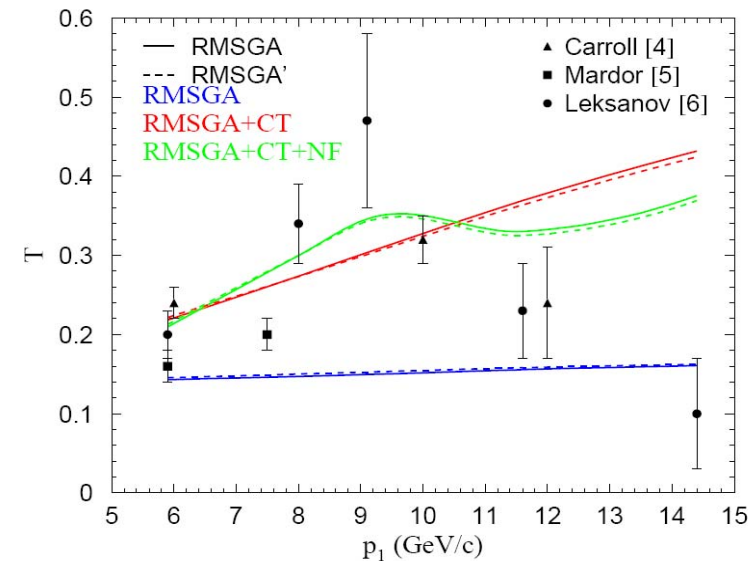
Fig. 1. The nuclear transparency for the ^{12}C$(p, 2p)$ reaction as a func
the incoming lab momentum p_1. The full RMSGA (solid lines) are comp
the RMSGA' (dashed lines) results. The different curves represent the R
RMSGA+CT and RMSGA+CT+NF calculations. The CT effects are cal
in the FLFS model [21] with $\Delta M^2 = 0.7$ (GeV/c^2)^2 and the results includ
mechanism of NF are obtained using the positive sign of $\phi(s) + \delta_1$. Data a
Refs. [4,5,6].

Energy Dependence of Nuclear Transparency in C(p,2p) Scattering

A. Leksanov,[5] J. Alster,[1] G. Asryan,[3,2] Y. Averichev,[8] D. Barton,[3] V. Baturin,[5,4] N. Bukhtoyarova,[3,4] A. Carroll,[3] S. Heppelmann,[5] T. Kawabata,[6] Y. Makdisi,[3] A. Malki,[1] E. Minina,[5] I. Navon,[1] H. Nicholson,[7] A. Ogawa,[5] Yu. Panebratsev,[8] E. Piasetzky,[1] A. Schetkovsky,[5,4] S. Shimanskiy,[8] A. Tang,[9] J. W. Watson,[9] H. Yoshida,[6] and D. Zhalov[5]

[1]School of Physics and Astronomy, Sackler Faculty of Exact Sciences, Tel Aviv University, Ramat Aviv 69978, Isra
[2]Yerevan Physics Institute, Yerevan 375036, Armenia
[3]Collider-Accelerator Department, Brookhaven National Laboratory, Upton, New York, 11973
[4]Petersburg Nuclear Physics Institute, Gatchina, St. Petersburg 188350, Russia
[5]Physics Department, Pennsylvania State University, University Park, Pennsylvania 16801
[6]Department of Physics, Kyoto University, Sakyoku, Kyoto, 606-8502, Japan
[7]Department of Physics, Mount Holyoke College, South Hadley, Massachusetts 01075
[8]J.I.N.R., Dubna, Moscow 141980, Russia
[9]Department of Physics, Kent State University, Kent, Ohio 44242
(Received 20 April 2001; published 6 November 2001)

The transparency of carbon for (p,2p) quasielastic events was measured at beam momenta ranging from 5.9 to 14.5 GeV/c at 90° c.m. The four-momentum transfer squared (Q^2) ranged from 4.7 to 12.7 (GeV/c)^2. We present the observed beam momentum dependence of the ratio of the carbon to hydrogen cross sections. We also apply a model for the nuclear momentum distribution of carbon to obtain the nuclear transparency. We find a sharp rise in transparency as the beam momentum is increased to 9 GeV/c and a reduction to approximately the Glauber level at higher energies.

$$T_{CH} = T \int d\alpha \int d^2\vec{P}_{FT}\, n(\alpha, \vec{P}_{FT}) \frac{\left(\frac{d\sigma}{dt}\right)_{pp}(s(\alpha))}{\left(\frac{d\sigma}{dt}\right)_{pp}(s_0)}$$

$$\alpha \equiv A \frac{(E_F - P_{Fz})}{M_A} \simeq 1 - \frac{P_{Fz}}{m_p}$$
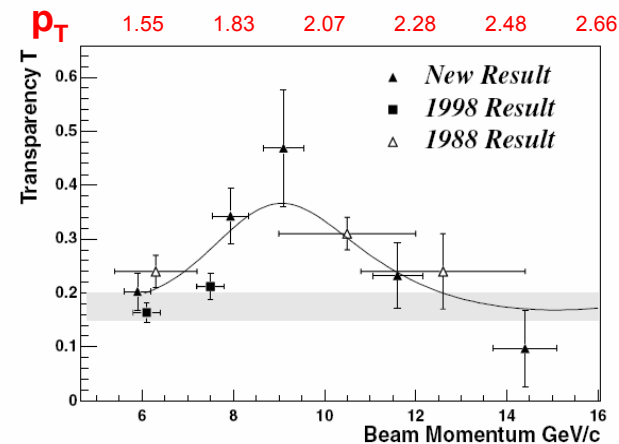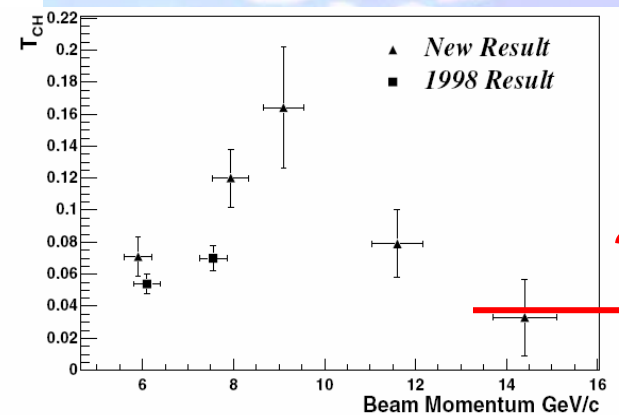
FIG. 2. Top: The transparency ratio T_{CH} as a function of the beam momentum for both the present result and two points from the 1998 publication [3]. Bottom: The transparency T versus beam momentum. The vertical errors shown here are all statistical errors, which dominate for these measurements. The horizontal errors reflect the α bin used. The shaded band represents the Glauber calculation for carbon [9]. The solid curve shows the shape R^{-1} as defined in the text. The 1998 data cover the c.m. angular region from 86°−90°. For the new data, a similar angular region is covered as is discussed in the text. The 1988 data cover 81°−90° c.m.

COLOR TRANSPARENCY

VIII. SUGGESTIONS FOR FUTURE EXPERIMENTS

Clearly there remain a number of interesting investigations involving nuclear transparency of protons and other hadrons. A revival of the AGS fixed target program [44], or the construction of the 50-GeV accelerator as part of the J-PARC complex in Japan [55], would provide excellent opportunities to expand the range of these nuclear transparency studies. Some of the remaining questions are the following.

(1) What happens at higher incident momentum? Does nuclear transparency rise again above 20 GeV/c, as predicted in the Ralston-Pire picture [56]?

(2) A-dependent studies in the 12 to 15 GeV/c range; will the effective absorption cross section continue to fall after the nuclear transparency stops rising at $\sim$9.5 GeV/c [56]?

(3) At the higher energy ranges of these experiments the spin effects are expected to be greatly diminished. However, they continue to persist, as shown in both single and double spin measurements [34,57]. So it is important to see, in quasielastic scattering inside a nucleus, whether a relatively pure pQCD state is selected, and if the spin dependent effects are attenuated.

(4) Measurements of nuclear transparency with antiprotons, pions, and kaons will be informative. These particles have widely different cross sections at $90^\circ_{c.m.}$. For instance, the pp differential cross section at $90^\circ_{c.m.}$ is 50 times larger than the $\bar{p}p$ differential cross section [19]. How should this small size of the $\bar{p}p$ cross section affect the absorption of $\bar{p}$'s by annihilation?

(5) The production of exclusively produced resonances provides a large testing ground for nuclear transparency effects. This is especially true for those resonances that allow the determination of final state spin orientation, such as ρ's or Λ's [19,36]. Will the interference terms that generate asymmetries disappear for reactions which take place in the nucleus?

(6) Measurements in light nuclei that determine the probability of a second hard scatter after the first hard interaction are an alternative way to study nuclear transparency effects. With the proper kinematics selected, the probability of the second scatter is dependent on the state of the hadrons at the first hard interaction [58].

High p_T suppression in AA-collisions
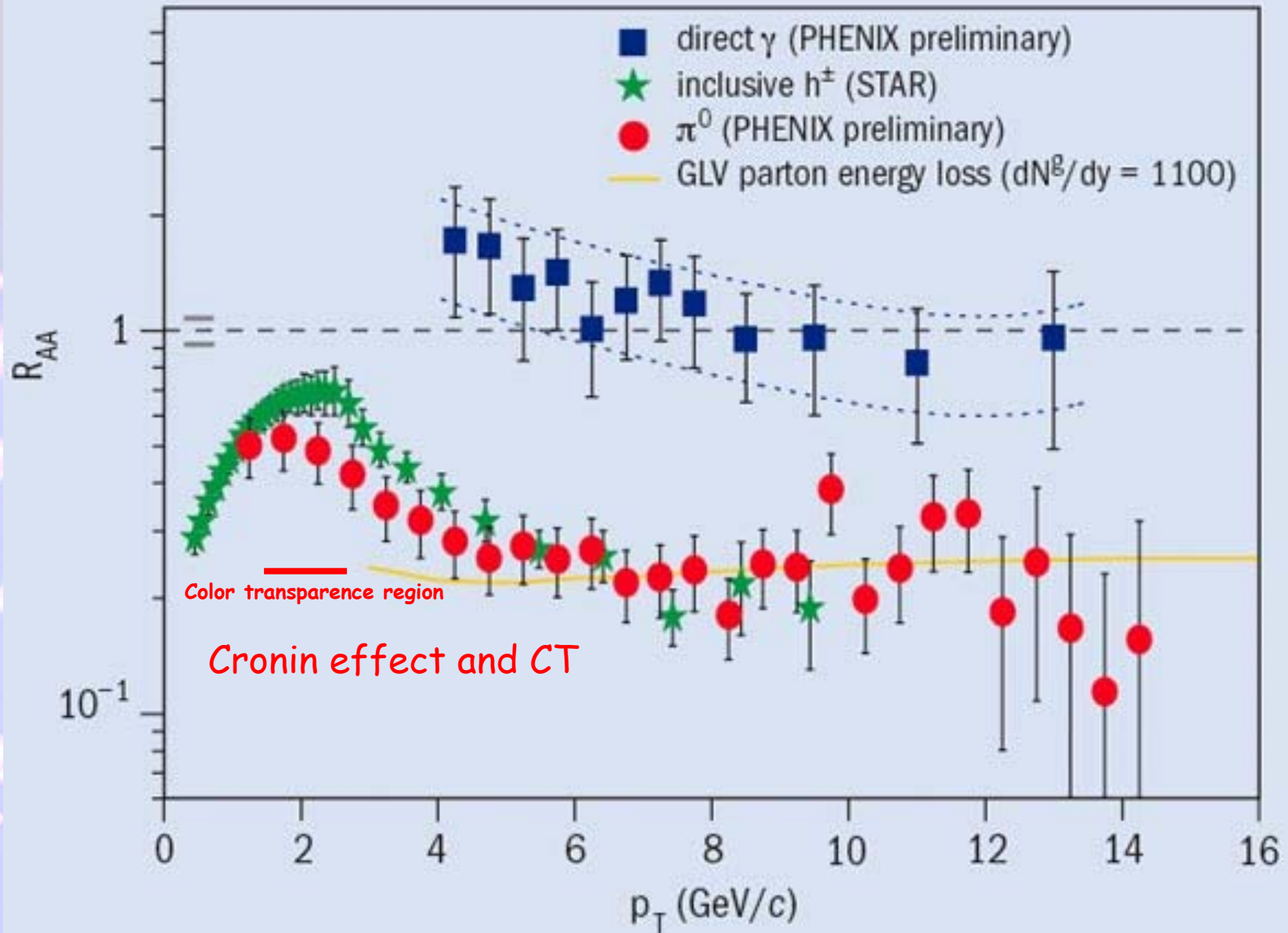
Legend:
- ■ direct γ (PHENIX preliminary)
- ★ inclusive h± (STAR)
- ● π⁰ (PHENIX preliminary)
- — GLV parton energy loss (dN^g/dy = 1100)

Color transparence region

Cronin effect and CT

RHIC news

Evidence for Color Transparency and Direct Hadron Production at RHIC [1]

By Stanley J. Brodsky

About the Author

Stan Brodsky is a Professor of Theroetical Physics at SLAC at Stanford University, and the winner of the 2007 J. J. Sakurai Prize of the American Physical Society. He is a Visiting Professor at Stony Brook University and a Visting Scientist at Brookhaven National Laboratory this fall and spring.

The QCD color transparency of higher-twist contributions to the inclusive hadroproduction cross section where the trigger proton is produced directly in a short-distance subprocess can explain several remarkable features of high-p_T proton production in heavy ion collisions which have recently been observed at RHIC: (a) the anomalous increase of the p $\rightarrow$ π ratio with centrality (b): the more rapid power-law fall-off at fixed x_T of the charged particle production cross section in high centrality nuclear collisions, and (c): the anomalous decrease of the number of same-side hadrons produced in association with a proton trigger as the centrality increases. These phenomena provide new perspectives for interpreting QCD processes in the nuclear medium.

Cumulative and Subthreshold particle production are very nice processes to investigate the high dense state of the cold nuclear matter.

Two theoretical ways to describe these phenomena:

• Fermi motion and SRC (will produce equal final QG phase for cold and hot evolution ways of nuclear matter)

• Fluctons will open new possibilities (quark stars, diquark condensate...)

$$(X_I \cdot M_I) + (X_{II} \cdot M_{II}) \rightarrow m_c + [X_I \cdot M_I + X_{II} \cdot M_{II} + m_2]$$

Quark-parton model

$$(X_I \cdot P_I) + (X_{II} \cdot P_{II}) \rightarrow M(X_I, X_{II})$$

P_I

A_I { X_I {

Cumulative particle

$S > S_0$

X_{II} {

A_{II} {

P_{II}
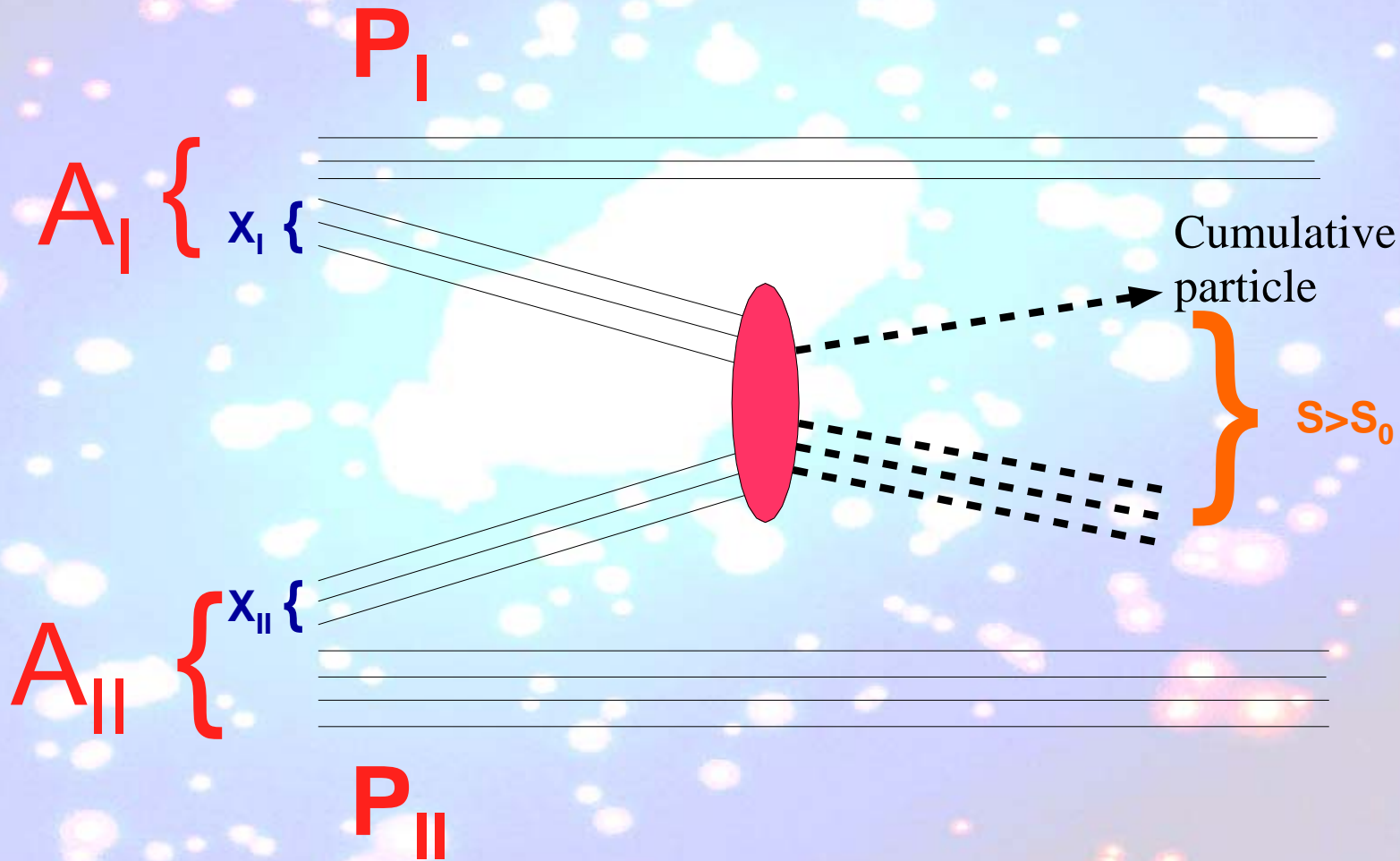
$$s_{\mathrm{cumulative}} = \left(X_I \cdot \frac{P_I}{A_I} + X_{II} \cdot \frac{P_{II}}{A_{II}}\right)^2$$

Cumulative and Subthreshold processes

$$S_{\mathrm{cumulative}} > S_0$$

$X_I \in [0, A_I]$ and $X_{II} \in [0, A_{II}]$

$X_I = X_{II} = 1$ - for   free NN-interaction

kinematical borders

$X_I > 1,$
$X_{II} > 1$

S_0 - kinemat.

$X_I > 1$

$X_{II} > 1$

y_0
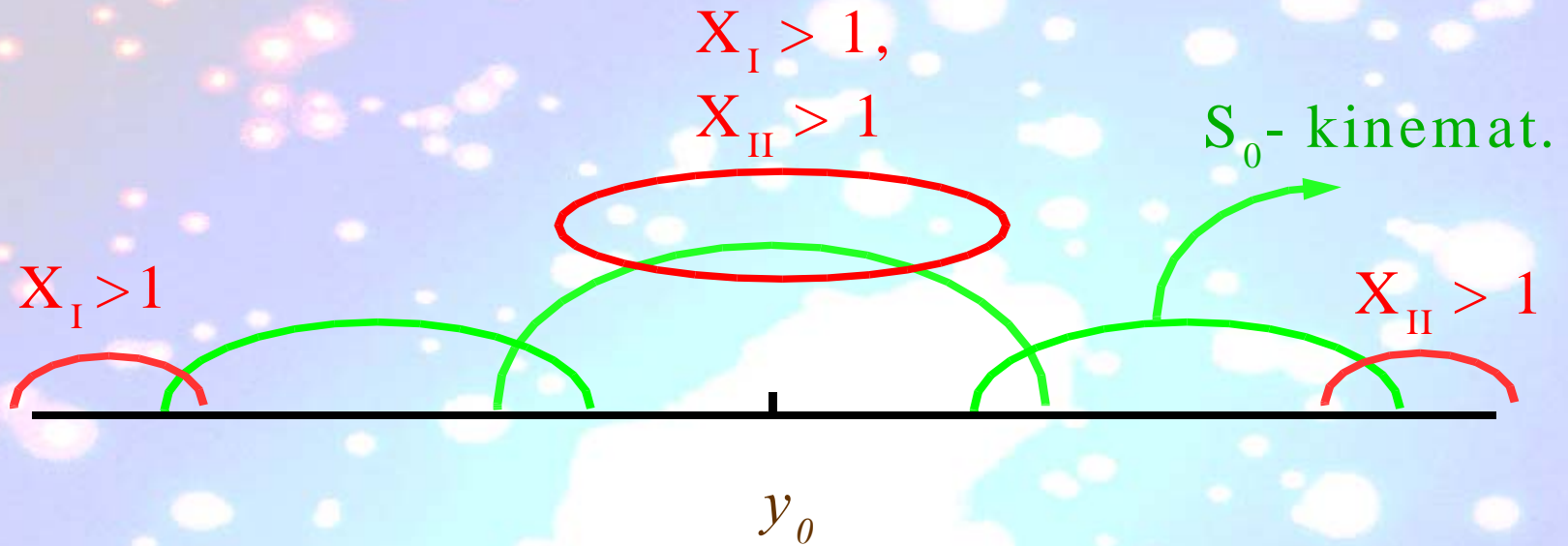
Cumulative processes:

1) X_I = 1 and X_{II} > 1 $\Big\}$ Fragmentation

2) X_{II} = 1 and X_I > 1 $\Big\}$ regions

3) X_I > 1 and X_{II} > 1   Central region

Fragmentation regions

$$\mu + N_{min} \cdot m \rightarrow m_c + [\, N_{min} \cdot m + \Delta\,]$$

$$\text{for } E_\mu \gg m_i \,, \; E_c$$

$$X = N_{\min} = Q \cong \frac{(E_c - \beta_\mu \cdot P_c \cdot \cos\theta_c)}{m} + \ldots \equiv X_I(X_{II}) \quad \text{Stavinsky (1970's)}$$

Common case for AA-collisions

V.S. Stavinsky JINR Rapid Communications N18-86, p.5 (1986)

$$(X_I \cdot M_I) + (X_{II} \cdot M_{II}) \rightarrow m_c + [X_I \cdot M_I + X_{II} \cdot M_{II} + m_2\,]$$

$$S_{\min}^{1/2} = \min(S^{1/2}) = \min[(X_I \cdot P_I + X_{II} \cdot P_{II})^{1/2}]$$

Stavinsky added new condition which fix X_I and X_{II}.

$$s_{min}^{1/2} = min(s^{1/2}) = min[(X_I^2 \cdot M_I^2 + X_{II}^2 \cdot M_{II}^2 + 2 \cdot X_I \cdot X_{II}(P_I \cdot P_{II}))^{1/2}]$$

For quak-parton models we don't have this condition
and will need to integrate over X_I and X_{II}.

In quark-parton models we take $M_I = M_2 = 0$. This is a
difference between Bjorken and Stavinsky variables X.
(What will connect with X mass or momentum?)

But may be in high p_T region we can use this condition for
quark-parton models too!?

Stavinsky's X connect with mass and flucton models.

Quasibinary reactions we can find in the region of
high p_T phenomenons.

ЕДИНЫЙ АЛГОРИТМ ВЫЧИСЛЕНИЯ ИНКЛЮЗИВНЫХ СЕЧЕНИЙ
РОЖДЕНИЯ ЧАСТИЦ С БОЛЬШИМИ ПОПЕРЕЧНЫМИ ИМПУЛЬСАМИ
И АДРОНОВ КУМУЛЯТИВНОГО ТИПА

В.С.Ставинский

Предложен единый алгоритм вычисления инклюзивных
сечений рождения частиц с большими поперечными импульсами и адронов кумулятивного типа. Возможность единого описания этих процессов обусловлена введением нового аргумента – минимальной энергии сталкивающихся конституентов, необходимой для рождения наблюдаемой частицы. Проведено сравнение с экспериментальными данными.

Работа выполнена в Лаборатории высоких энергий ОИЯИ.

Unique Algorithm for Calculation of Inclusive
Cross Sections of Particle Production
with Big Transverse Momenta and of Cumulative
Type Hadrons

V.S.Stavinskij

Unique algorithm is proposed for calculating inclusive cross sections of particle production with big transverse momenta and cumulative type hadrons. A possibility of unique description of these processes is due to introduction of a new argument – of minimal energy of colliding constituents needed for the production of observed particle.

The investigation has been performed at the Laboratory of High Energies, JINR.
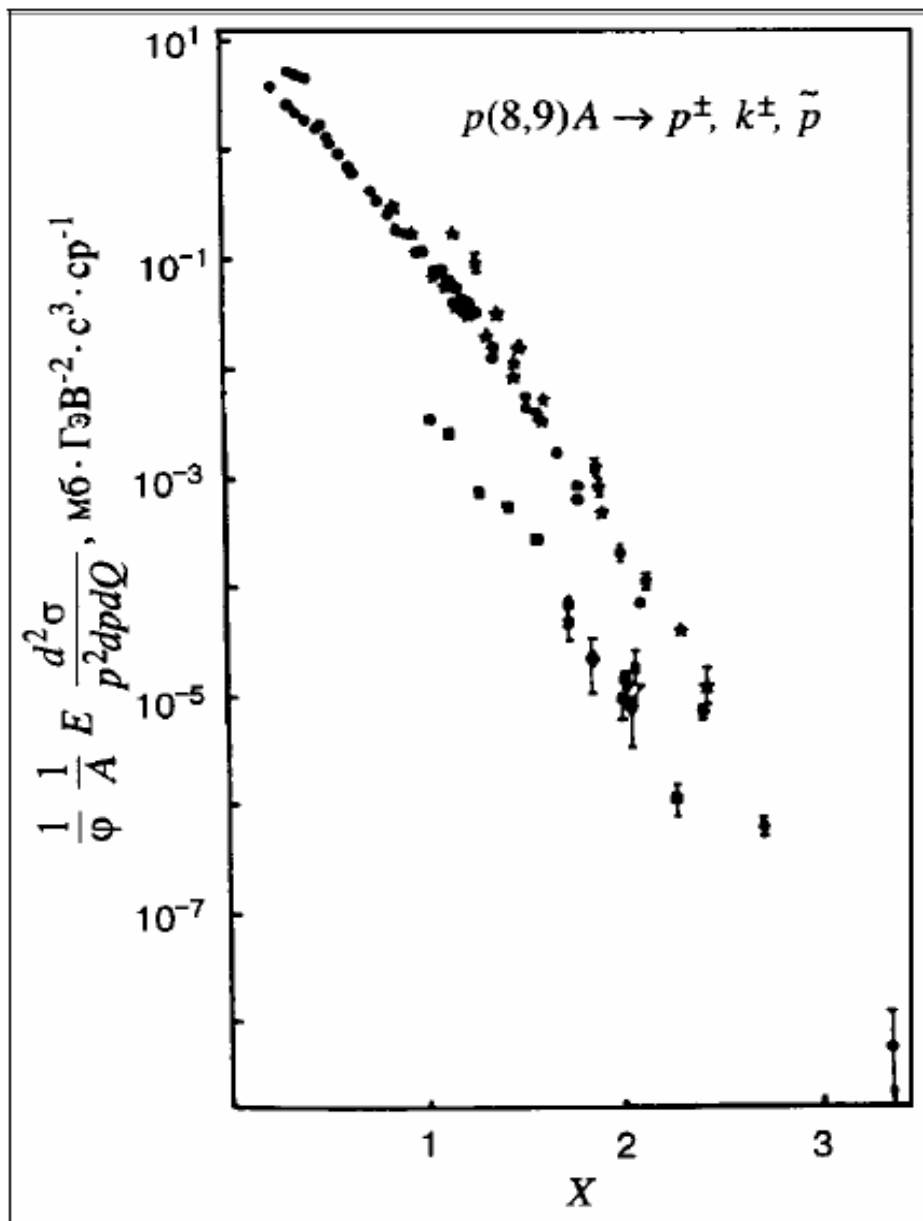
Рис.10. Экспериментальные данные, полученные группой В.С.Ставинского, по кумулятивному рождению пионов, каонов и антипротонов в зависимости от введенного им параметра X

ВОЗМОЖЕН ЛИ ЕДИНЫЙ ПОДХОД К ПОДПОРОГОВЫМ И КУМУЛЯТИВНЫМ ПРОЦЕССАМ В РЕЛЯТИВИСТСКИХ ЯДЕРНЫХ СТОЛКНОВЕНИЯХ?

А.А.Балдин*

Предлагается единый подход к описанию подпороговых, кумулятивных и дважды кумулятивных процессов на основе гипотезы об автомодельности релятивистских ядерных столкновений. Расчеты, проведенные в рамках предложенной модели, сравниваются с разнообразными экспериментальными данными.

Работа выполнена в Институте ядерных исследований РАН, Москва.

Is the Universal Approach to the Subthreshold and Cumulative Processes in Relativistic Nuclear Collisions Possible?

A.A.Baldin

The universal approach to the description of subthreshold, cumulative and twice-cumulative processes based on the self-similarity hypothesis is presented and applied to the various reactions. Large experimental material including nucleus-nucleus and proton-nucleus interactions is analyzed.

The investigation has been performed at the Institute for Nuclear Research, Russian Academy of Sciences, Moscow

A.A. Baldin's parameterization

$$\Pi = \frac{1}{2}(X_I^2 + X_{II}^2 + 2 \cdot X_I \cdot X_{II} \cdot \gamma_{I,II})^{\frac{1}{2}} = \frac{1}{2 \cdot m} \cdot S_{min}^{\frac{1}{2}}$$

$$\gamma_{I,II} = \frac{(P_I \cdot P_{II})}{M_I \cdot M_{II}}$$

Inclusive data parameterization

$$E \cdot \frac{d^3\sigma}{dp^3} = C_1 \cdot A_I^{\frac{1}{3}+\frac{X_I}{3}} \cdot A_{II}^{\frac{1}{3}+\frac{X_{II}}{3}} \cdot \exp(-\frac{\Pi}{C_2}),$$

$$C_1 = 2200[mb \cdot GeV^{-2} \cdot c^3 \cdot sr^{-1}], C_2 = 0.127$$

A.A. Baldin's parameterization for cumulative and subthreshold particle production
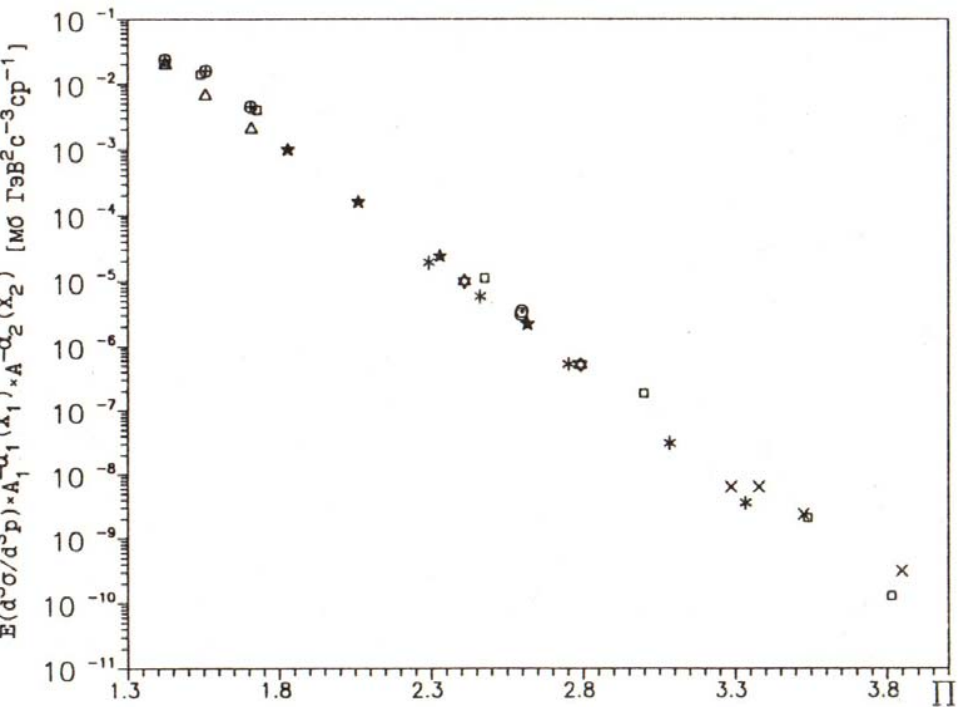
рис.1. Зависимость инвариантных дифференциальных сечений, деленных на $A_1^{\alpha_1(X_1)} A_2^{\alpha_2(X_2)}$, где $\alpha_1(X_1) = 2/3 + X_1/3$ и $\alpha_2(X_2) = 2/3 + X_2/3$, от параметра Π для следующих реакций: * Si + Si → K^- 2,0 ГэВ/нуклон, 0°[9]; × Si + Si → $\bar{p}$ 2,0 ГэВ/нуклон, 0°[9]; ✿ Si + Si → K^- 1,4 ГэВ/нуклон, 0°[8] о C + C → $\bar{p}$ 3,65 ГэВ/нуклон, 24°[11]; о d + C → $\bar{p}$ 3,65 ГэВ/нуклон, 24°[11]; ⊕ C + C → K^- 2,5—3,65 ГэВ/нуклон, 24°[12]; △ d + C → K^- 2,5—3,65 ГэВ/нуклон, 24°[12]; * p + C → K^- 9,2 ГэВ/нуклон, 119°[6]; □ p + C → π^- 9,2 ГэВ/нуклон, 119°[7]

Реакция	Екин. ГэВ/н	Лаб. имп. ГэВ/с	Лаб. угол вылет	$\sigma_{экс} = \dfrac{E}{p^2} \times \dfrac{d^2\sigma}{dp \times d\Omega}$ мб/ср ГэВ²/с³	$\sigma_{рас} = \dfrac{E}{p^2} \times \dfrac{d^2\sigma}{dp \times d\Omega}$ мб/ср ГэВ²/с³	Ссылка
d+C →$\bar{p}$	3.65	0.8	24°	$(1.5\pm0.6)\times10^{-4}$	9.3×10^{-5}	11
C+C →$\bar{p}$	3.65	0.8	24°	$(1.2\pm0.3)\times10^{-3}$	7.4×10^{-4}	11
C+Cu→$\bar{p}$	3.65	0.8	24°	$(6.2\pm2.0)\times10^{-3}$	6.05×10^{-3}	11
S1+S1→$\bar{p}$	2.0	1.0	0°	$(8.71\pm2.9)\times10^{-5}$	1.98×10^{-4}	9
S1+S1→$\bar{p}$	2.0	1.5	0°	$(1.03\pm0.25)\times10^{-4}$	1.2×10^{-4}	9
S1+S1→$\bar{p}$	2.0	1.9	0°	$(4.9\pm1.0)\times10^{-5}$	5.07×10^{-5}	9
S1+S1→$\bar{p}$	1.65	1.5	0°	$(1.41\pm0.38)\times10^{-5}$	9.1×10^{-6}	9
d+C→k^-	2.5	0.8	24°	$(4.1\pm2.0)\times10^{-2}$	5.7×10^{-2}	12
C+C→k^-	2.5	0.8	24°	$(4.6\pm1.0)\times10^{-1}$	4.4×10^{-1}	12
S1+S1→k^-	1.0	1.0	0°	$(1.2\pm1.5)\times10^{-3}$	1.1×10^{-3}	8
S1+S1→k^-	1.26	1.0	0°	$(8.0\pm5.0)\times10^{-3}$	2.26×10^{-2}	8
S1+S1→k^-	1.4	1.0	0°	$(5.0\pm1.5)\times10^{-2}$	7.0×10^{-2}	8
S1+S1→k^-	1.4	1.5	0°	$(5.0\pm1.5)\times10^{-3}$	7.56×10^{-3}	8
S1+S1→k^-	2.0	2.37	0°	$(1.5\pm1.0)\times10^{-2}$	1.66×10^{-2}	9
S1+S1→k^-	2.0	1.5	0°	$(2.5\pm0.5)\times10^{-1}$	3.46×10^{-1}	9
S1+S1→k^-	2.0	1.0	0°	$(1.5\pm0.5)\times10^{-3}$	1.45×10^{0}	9

ТЕОРИЯ

LARGE MOMENTUM PION PRODUCTION IN PROTON NUCLEUS COLLISIONS AND THE IDEA OF "FLUCTUONS" IN NUCLEI

V.V. BUROV

The Moscow State University, Moscow, USSR

and

V.K. LUKYANOV and A.I. TITOV

Joint Institute for Nuclear Research, Dubna, USSR

It is shown that in proton-nucleus collisions, the production of pions with large momenta can be explained by the assumption of the existence of nuclear density fluctuations ("fluctuons") at short distances of the nucleon core radius order, with the mass of several nucleons.

The purpose of this note is to realize the idea [4] that the cumulative effect is connected largely with a suggestion on the existence in nuclei of the so-called fluctuons. Earlier fluctuons were proposed [7] in order to understand the nature of the "deuteron peak" in the pA-scattering cross section at large momentum transfers [8] and also to interpret the pd-scattering cross section [9]. Compressional fluctuations of mass $M_k = km_p$ of nucleons in the small volume $V_\xi = \frac{4}{3}\pi r_\xi^3$ where r_ξ is the fluctuon radius were assumed.
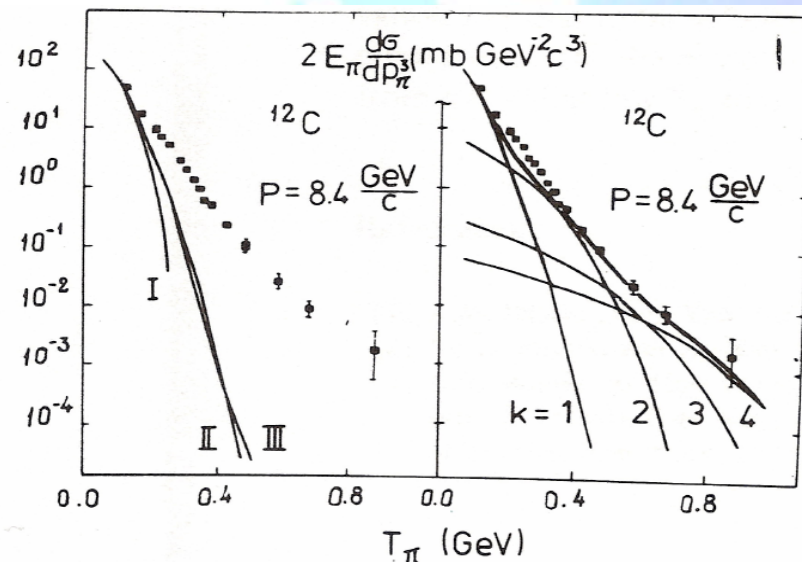
Fig. 1. (a) Calculations of the invariant pion production cross section for ^{12}C: I — for the free proton target; II — with fermi motion; III — the relativization effect. (b) The contributions of separate fluctuons with mass $M_k = km_p$ where k is the order of cumulativity.

Forward K^+ Production in Subthreshold pA Collisions at 1.0 GeV

V. Koptev,[1] M. Büscher,[2] H. Junghans,[2] M. Nekipelov,[1,2] K. Sistemich,[2] H. Ströher,[2] V. Abaev,[1] H.-H. Adam,[3] R. Baldauf,[4] S. Barsov,[1] U. Bechstedt,[2] N. Bongers,[2] G. Borchert,[2] W. Borgs,[2] W. Bräutigam,[2] W. Cassing,[5] V. Chernyshev,[6] B. Chiladze,[7] M. Debowski,[8] J. Dietrich,[2] M. Drochner,[4] S. Dymov,[9] J. Ernst,[10] W. Erven,[4] R. Esser,[11,*] P. Fedorets,[6] A. Franzen,[2] D. Gotta,[2] T. Grande,[2] D. Grzonka,[2] G. Hansen,[12] M. Hartmann,[2] V. Hejny,[2] L. v. Horn,[2] L. Jarczyk,[13] A. Kacharava,[9] B. Kamys,[13] A. Khoukaz,[3] T. Kirchner,[8] S. Kistryn,[13] F. Klehr,[12] H. R. Koch,[2] V. Komarov,[9] S. Kopyto,[2] R. Krause,[2] P. Kravtsov,[1] V. Kruglov,[9] P. Kulessa,[2,15] A. Kulikov,[9,14] V. Kurbatov,[9] N. Lang,[3] N. Langenhagen,[8] I. Lehmann,[2] A. Lepges,[2] J. Ley,[11] B. Lorentz,[2] G. Macharashvili,[7,9] R. Maier,[2] S. Martin,[2] S. Merzliakov,[9] K. Meyer,[2] S. Mikirtychiants,[1] H. Müller,[8] P. Munhofen,[2] A. Mussgiller,[2] V. Nelyubin,[1] M. Nioradze,[7] H. Ohm,[2] A. Petrus,[9] D. Prasuhn,[2] B. Prietzschk,[8] H. J. Probst,[2] D. Protic,[2] K. Pysz,[15] F. Rathmann,[2] B. Rimarzig,[8] Z. Rudy,[13] R. Santo,[3] H. Paetz gen. Schieck,[11] R. Schleichert,[2] A. Schneider,[2] Chr. Schneider,[8] H. Schneider,[2] G. Schug,[2] O. W. B. Schult,[2] H. Seyfarth,[2] A. Sibirtsev,[2] J. Smyrski,[13] H. Stechemesser,[12] E. Steffens,[16] H. J. Stein,[2] A. Strzalkowski,[13] K.-H. Watzlawik,[2] C. Wilkin,[17] P. Wüstner,[4] S. Yashenko,[9] B. Zalikhanov,[9] N. Zhuravlev,[9] P. Zolnierczuk,[13] K. Zwoll,[4] and I. Zychor[18]

K^+-meson production in pA (A = C, Cu, Au) collisions has been studied using the ANKE spectrometer at an internal target position of the COSY-Jülich accelerator. The complete momentum spectrum of kaons emitted at forward angles, $\vartheta \leq 12°$, has been measured for a beam energy of $T_p = 1.0$ GeV, far below the free NN threshold of 1.58 GeV. The spectrum does not follow a thermal distribution at low kaon momenta and the larger momenta reflect a high degree of collectivity in the target nucleus.
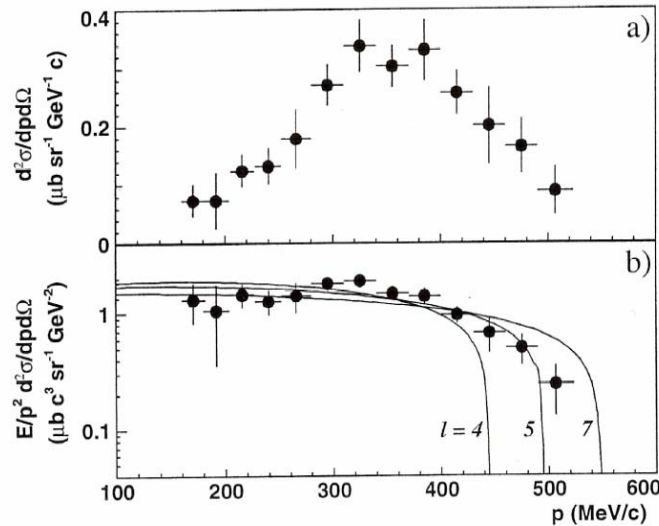
FIG. 2. (a) Double differential K^+-production cross section for the $p(1.0$ GeV$)^{12}$C $\rightarrow K^+(\vartheta \leq 12°)X$ reaction as a function of the K^+ momentum. (b) Same data plotted as invariant cross section. The error bars are purely statistical. The overall normalization uncertainty is estimated to be 10%. The solid lines describe the behavior of the invariant cross section within a phase-space approximation [Eq. (2)].

Subthreshold Antiproton Production in ^{28}Si + ^{28}Si Collisions at 2.1 GeV/Nucleon

J. B. Carroll,[1] S. Carlson,[1] J. Gordon,[1] T. Hallman,[4] G. Igo,[1] P. Kirk,[5] G. F. Krebs,[3] P. Lindstrom,[3] M. A. McMahan,[3] V. Perez-Mendez,[3] A. Shor,[2] S. Trentalange,[1] and Z. F. Wang[1]

[1]University of California at Los Angeles, Los Angeles, California 90024
[2]Brookhaven National Laboratory, Upton, New York, 11973
[3]Lawrence Berkeley Laboratory, Berkeley, California 94720
[4]Johns Hopkins University, Baltimore, Maryland 21218
[5]Louisiana State University, Baton Rouge, Louisiana 70803
(Received 12 December 1988; revised manuscript received 16 February 1989)

We report on the first observation of subthreshold antiproton production in nucleus-nucleus collisions. This measurement was made for the system ^{28}Si + ^{28}Si at a bombarding energy of 2.1 GeV/nucleon (kinetic energy per NN pair in the c.m. frame $\sim$850 MeV). A differential cross section $d^2\sigma/dP\,d\Omega$ of 80 ± 40 nb/sr (GeV/c) was measured for $\bar{p}$ production at 1.9 GeV/c and 0°. This result is 3 orders of magnitude larger than that predicted by a calculation incorporating internal motion of the nucleons in the colliding nuclei.
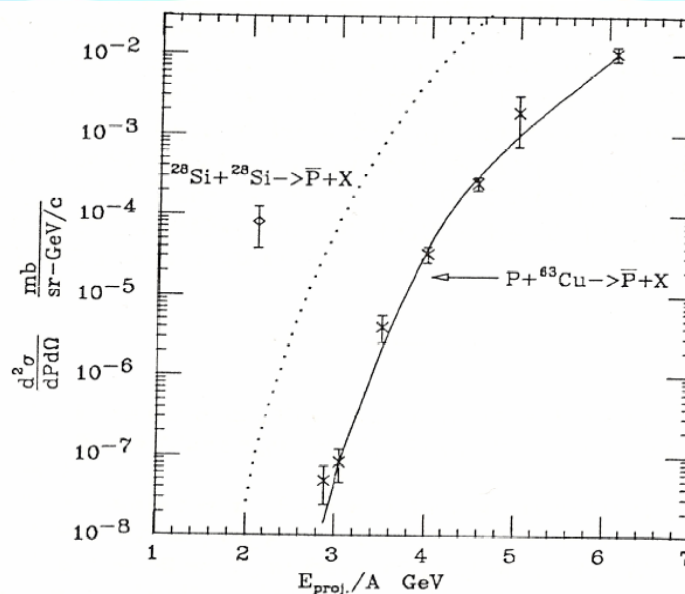
FIG. 3. Subthreshold antiproton production in p + Cu collisions ($\times$) and a comparison with $\bar{p}$ production in Si+Si collisions ($\diamond$). Solid line is a calculation for p + Cu $\to \bar{p}$ + X incorporating a double-Gaussian distribution for the internal nuclear momentum (Ref. 11). Dotted line is the same calculation for Si+Si $\to \bar{p}$ + X.

Fermi motion or Short Range Correlation (SRC) mechanism
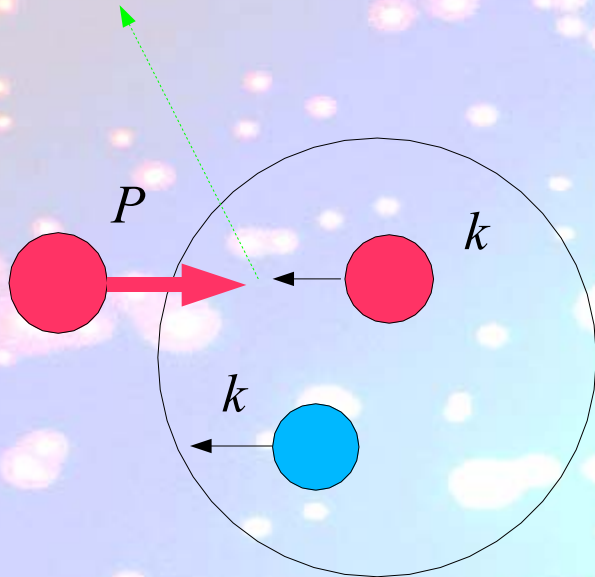
$$p + A \to \pi, \kappa, \overline{p}, \dots + X$$

$$\sigma_\pi \sim n(\vec{k}) \cdot \sigma(NN \to \pi, K + X)$$
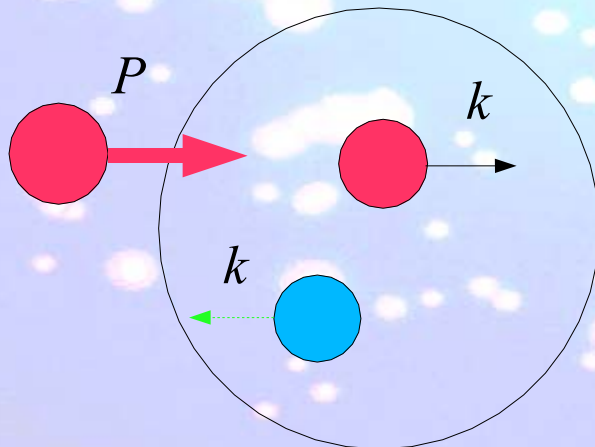
$$p + A \to n, p, \dots + X$$

$$\sigma_N \sim n(\vec{k}) \cdot \sigma_0$$

Flucton hypothesis

$$p + A \rightarrow \pi, \kappa, \bar{p}, p, n, ... + X$$

$$\sigma_h \sim P_K \cdot G_{h/K}(K)$$

ОБЗОРЫ
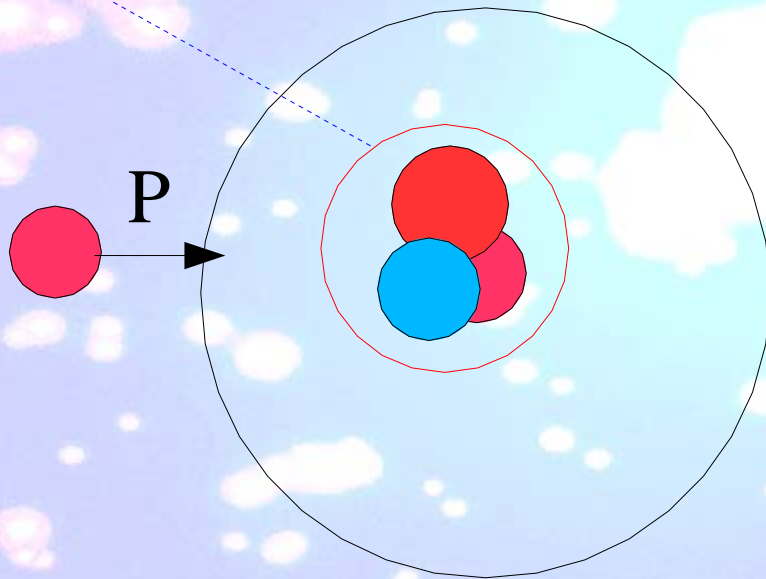
ПУТИ ИССЛЕДОВАНИЯ ЯДЕРНОГО ВЕЩЕСТВА В УСЛОВИЯХ, ХАРАКТЕРНЫХ ДЛЯ ЕГО ПЕРЕХОДА В КВАРК-ГЛЮОННУЮ ПЛАЗМУ

© 2002 г.   Г. А. Лексин

Институт теоретической и экспериментальной физики, Москва, Россия
Поступила в редакцию 07.02.2002 г.

Кратко представлены свойства глубоконеупругих ядерных реакций, происходящих на плотных флуктуациях ядерной материи (флуктонах). Обсуждаются свойства флуктонов, которыми могут быть многокварковые "мешки" или "капельки" кварк-глюонной плазмы: характерные параметры ядерного вещества во флуктоне — "температура" и плотность порядка критических для фазового перехода. Их значения могут быть достигнуты или превзойдены, если выделить события флуктон-флуктонных столкновений. Обсуждается способ выделения.

2044
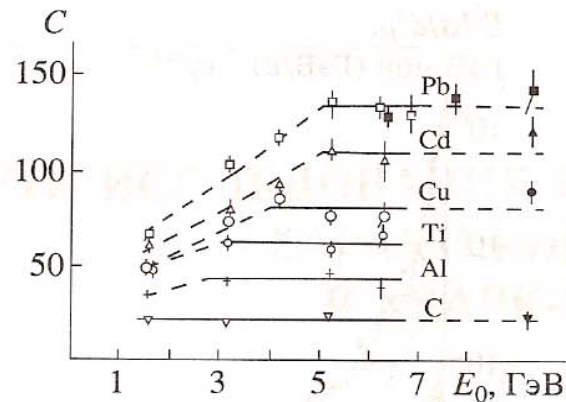
Рис. 3. Зависимость коэффициента $C(T_0 = 125$ МэВ$)$ в параметризации инвариантной функции $f = C \times \times \exp(-T/T_0)$ в реакции $pA(\text{C, Al, Ti, Cu, Cd, Pb}) \rightarrow \rightarrow pX$ для угла вылета протонов $120°$ в л.с. от энергии налетающих протонов. Черные точки справа относятся к начальной энергии 400 ГэВ.
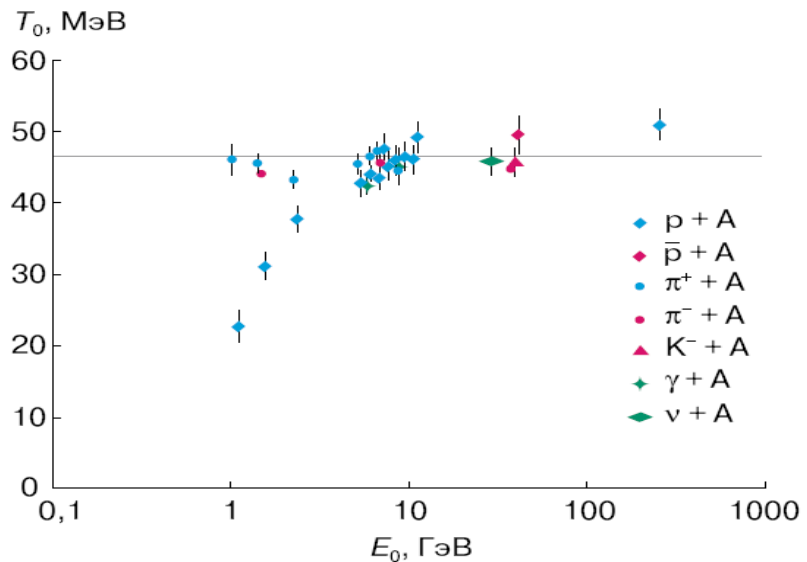
Рис. 3. Зависимость наклонов инвариантных функций кумулятивных протонов, вылетающих под углом $120°$, от энергии различных налетающих частиц.

Energy Dependence of Charged Pions Produced at 180° in 0.8–4.89-GeV Proton-Nucleus Collisions

L. S. Schroeder, S. A. Chessin, J. V. Geaga, J. Y. Grossiord,[a]
J. W. Harris, D. L. Hendrie, R. Treuhaft, and K. Van Bibber
Lawrence Berkeley Laboratory, University of California, Berkeley, California 94720
(Received 25 September 1979)

High-energy charged pions produced at 180° in 0.8–4.89-GeV proton-nucleus collisions have been studied. Both the slopes of the energy spectra and the π^-/π^+ ratios increase rapidly with primary energy up to ~ 3–4 GeV, where limiting values appear to be reached. The dependence on target mass also changes over this energy range. Unlike forward pion-production results, backward pions at these energies do not obey the scaling law suggested by Schmidt and Blankenbecler.

We report on a systematic study of the energy dependence of charged pions produced at 180° in the collisions of 0.8–4.89-GeV protons with nuclei. A principal reason for studying production of energetic pions from nuclei in the backward direction is that in free nucleon-nucleon (N–N)

collisions such production is kinematically restricted. Observation of pions beyond this kinematic limit may then be evidence for exotic production mechanisms such as production from clusters.[1-5] Early experiments by Baldin et al.[6] using 5.14- and 7.52-GeV protons observed
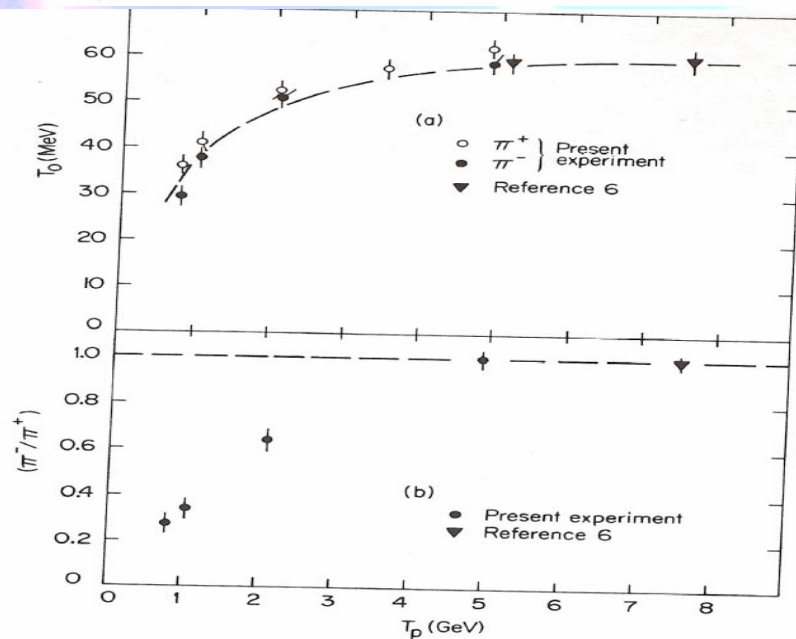
FIG. 1. Energy dependence of (a) T_0 parameter for pions, and (b) the π^-/π^+ ratio at 180° obtained by integrating each spectra up to 100 MeV for p-Cu collisions from 0.8 to 4.89 GeV. The dashed curve in both cases refers to the predictions of the "effective-target" model (Refs. 3 and 4).

tering mechanism to one where nucleon clusters play an ever increasing role. To isolate the production mechanism further, experiments are required which will measure additional observables such as associated multiplicities and two-particle correlations. However, it is clear that by measuring the production of pions in kinematic regions beyond those available in free N-N collisions, such as at 180° and high energies, one is probing the short-range behavior of nucleons in nuclei. This behavior might manifest itself as large Fermi momenta or nucleon clusters.

f, мб · ГэВ$^{-2}$ · c^3 · ср$^{-1}$ · нуклон$^{-1}$

- π^-, 119°
- π^+, 119°
- K^+, 119°
- K^-, 119°
- p, 119°
- $\overline{p}$, 119°
- $\overline{p}$, 97°

$\alpha = (E - p\cos\theta)/m_n$

p, ГэВ/c
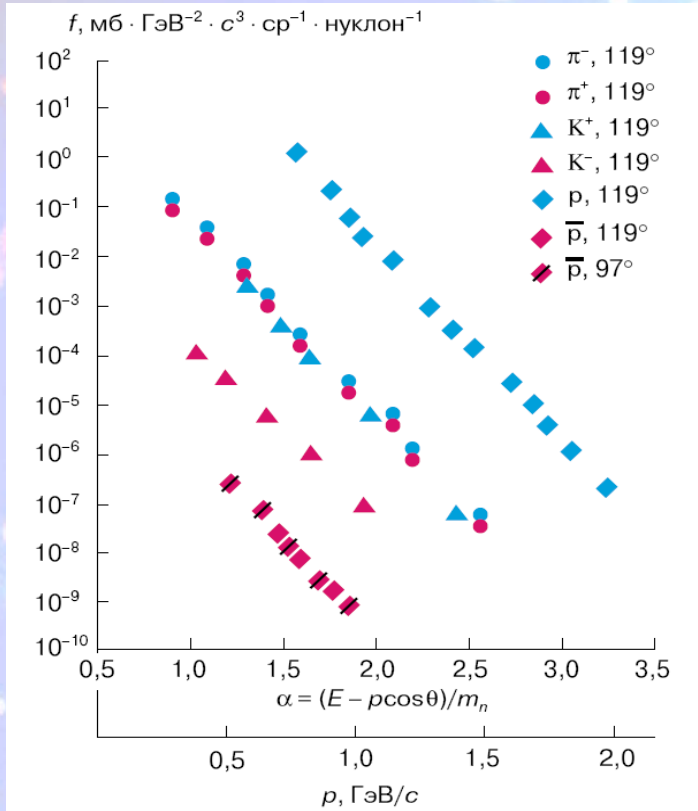
Рис. 2. Зависимость инвариантных функций различных кумулятивных частиц от их величин α. Нижняя шкала абсцисс – импульс кумулятивных протонов при соответствующем α.

f_n/f_p

n/p

pPb πPb d/u

pU πU

n/p

d/u

T_N, МэВ
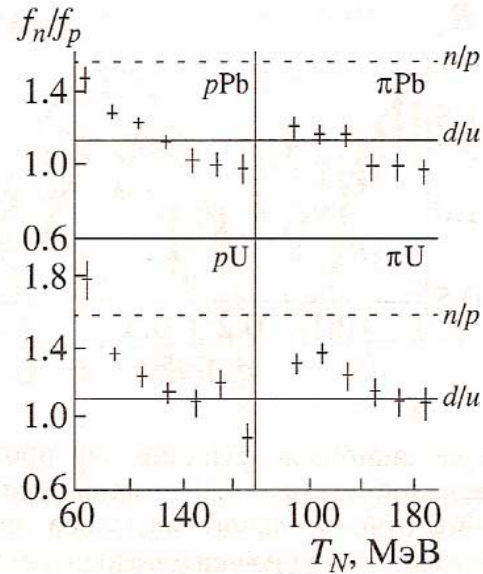
Рис. 12. Отношение выходов нейтронов к протонам из изонесимметричных ядер Pb и U в зависимости от кинетической энергии вылетающих нуклонов; угол вылета 120°, начальная энергия протонов 7.5 ГэВ и пионов 5 ГэВ. Данные, полученные под действием $\pi^{\pm}$-мезонов, усреднены. Штриховые линии — отношение нейтронов к протонам в ядрах мишени, сплошные — отношение d/u-кварков в ядрах Pb и U.

КУМУЛЯТИВ

Pion production: A probe for coherence in medium-energy heavy-ion collisions

J. Stachel, P. Braun-Munzinger, R. H. Freifelder,* P. Paul, S. Sen, P. DeYoung,† and P. H. Zhang‡
Department of Physics, State University of New York at Stony Brook, Stony Brook, New York 11794

T. C. Awes, F. E. Obenshain, F. Plasil, and G. R. Young
Physics Division, Oak Ridge National Laboratory, Oak Ridge, Tennessee 37831

R. Fox and R. Ronningen
*National Superconducting Cyclotron Laboratory, Michigan State University,
East Lansing, Michigan 48824*
(Received 19 November 1985)

The production of neutral pions has been studied in reactions of 35 MeV/nucleon ^{14}N$+^{27}$Al,Ni,W and 25 MeV/nucleon ^{16}O$+^{27}$Al,Ni. Inclusive pion differential distributions $d\sigma/dT_\pi$, $d\sigma/d\Omega$, $d\sigma/dy$, $d\sigma/dp_\perp$, and $d^2\sigma/dy\,dp_\perp$ have been measured by detecting the two pion-decay γ rays in a setup of 20 lead glass Čerenkov detector telescopes. Special care was taken to understand and suppress background events. Effects of pion reabsorption are discussed and it is found that the cross sections presented here are substantially affected by such final state interactions. The comparatively large experimental cross sections and the shape of the spectral distributions cannot be accounted for in single nucleon-nucleon collision or statistical models; they rather call for a coherent pion production mechanism.
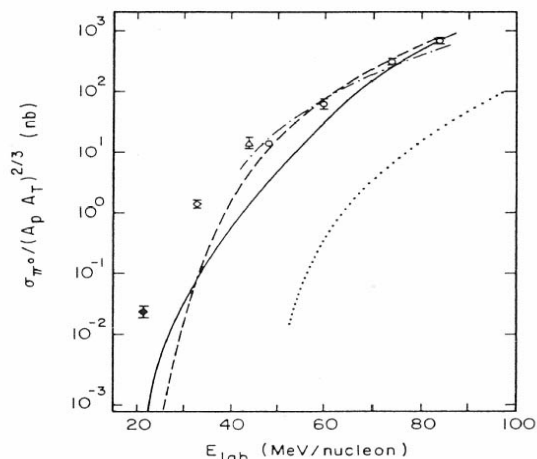
FIG. 13. Experimental integrated pion production cross sections divided by $(A_P A_T)^{2/3}$ for different beam energies. The different symbols signify ^{16}O + ^{27}Al,Ni (closed diamond, present data), ^{14}N+^{27}Al,Ni,W (open diamond, present data), ^{40}Ar + ^{40}Ca (open triangle, Ref. 9), and ^{12}C + ^{12}C (open circles, Refs. 8 and 10). Also shown are results of a single nucleon-nucleon hard scattering model (Ref. 23) (dotted line), the extended phase space model (Ref. 27) (dashed line), a thermal model (Ref. 30) (solid line), and the bremsstrahlung model (Ref. 38) (dashed dotted line).
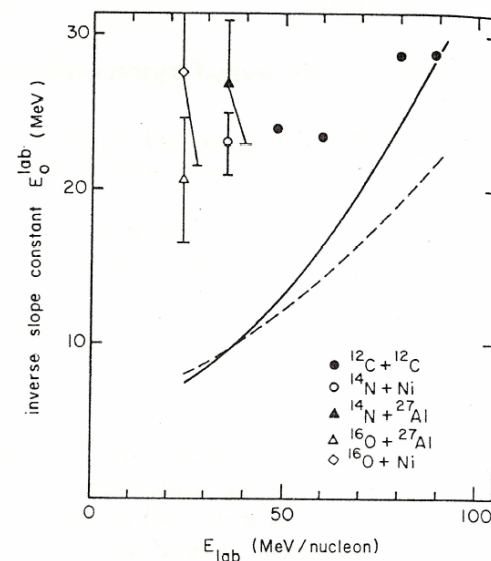
FIG. 14. Experimentally determined slope constants E_0 of pion kinetic energy spectra plotted as a function of beam energy/nucleon. For C + C spectra see Refs. 8 and 10. The solid and dashed lines correspond to predictions of Refs. 30 and 27, respectively. For details see the text.

Subthreshold particleproduction in to the flucton-flucton mechanism
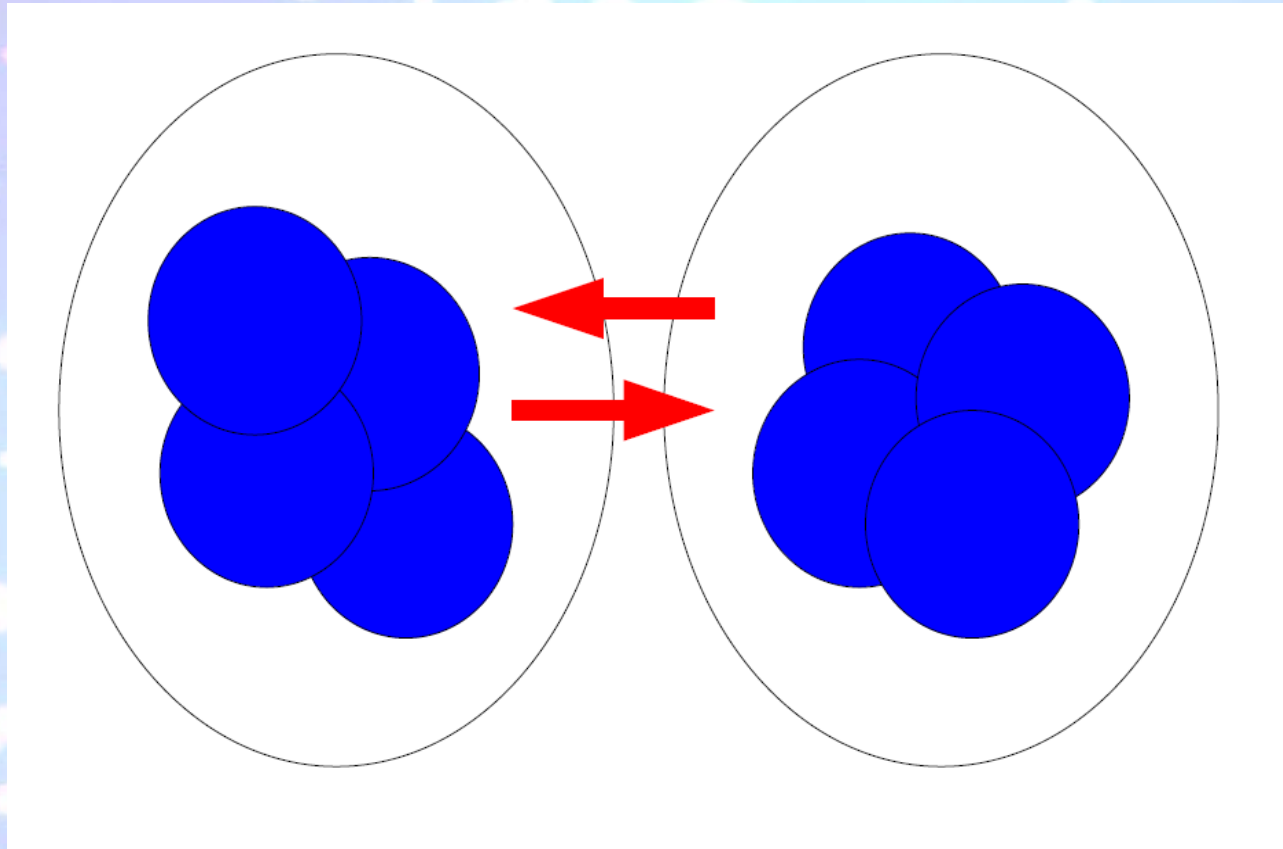
$$\sigma_h \sim P^2{}_K \cdot G^2{}_{h/K}(K)$$

Inverse slope for subthreshold production must be the less then $T_0/2$
(near the phase space border).
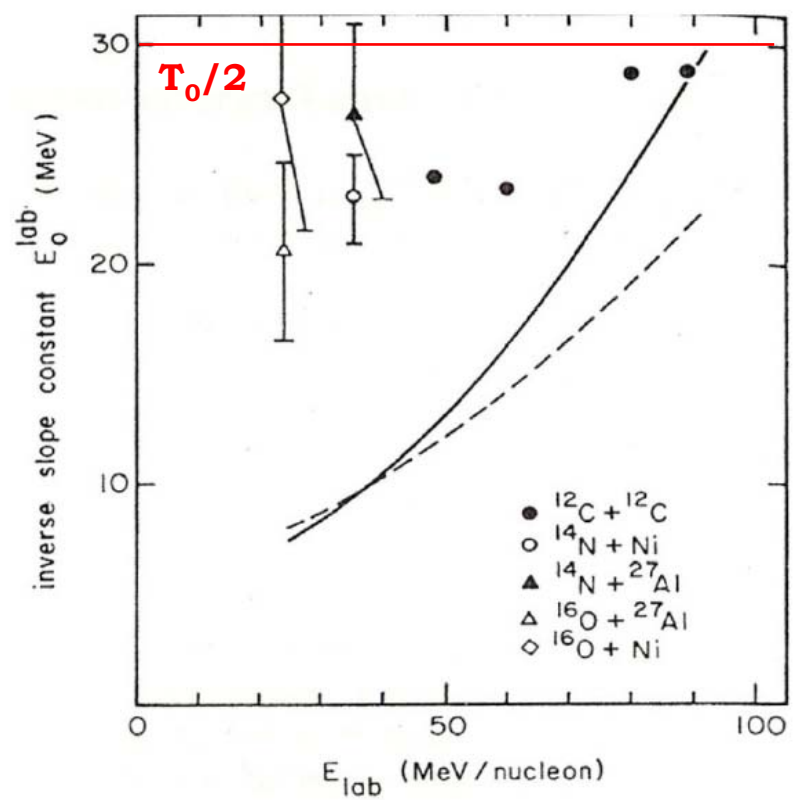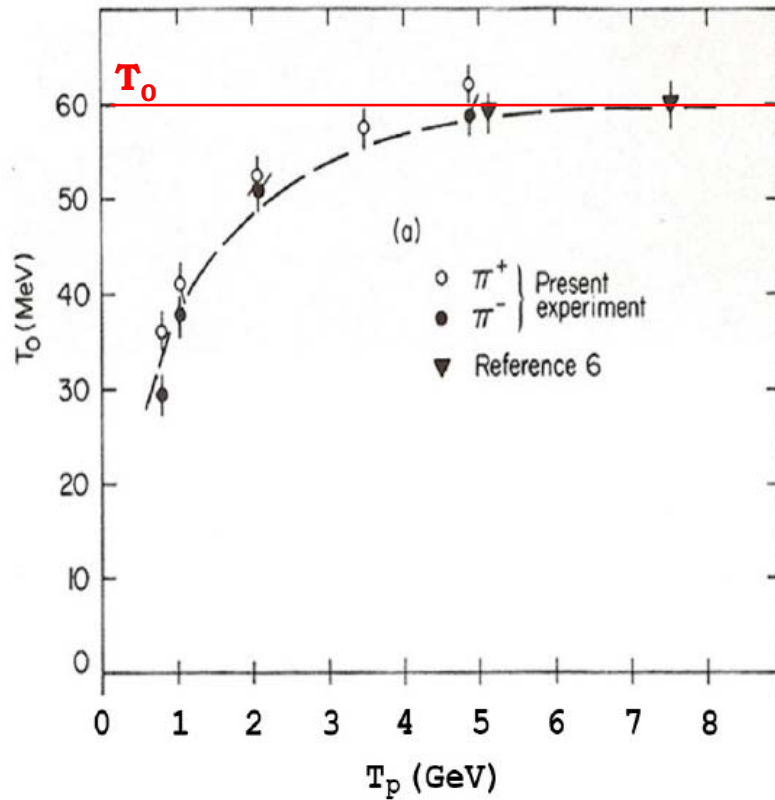
$$P_{cum} \sim \exp\left(-T/T_0\right) \quad \Rightarrow \quad P_{subthresh} \sim \exp\left(-T/T_0\right) \cdot \exp\left(-T/T_0\right) \sim \exp\left(-T/(T_0/2)\right)$$
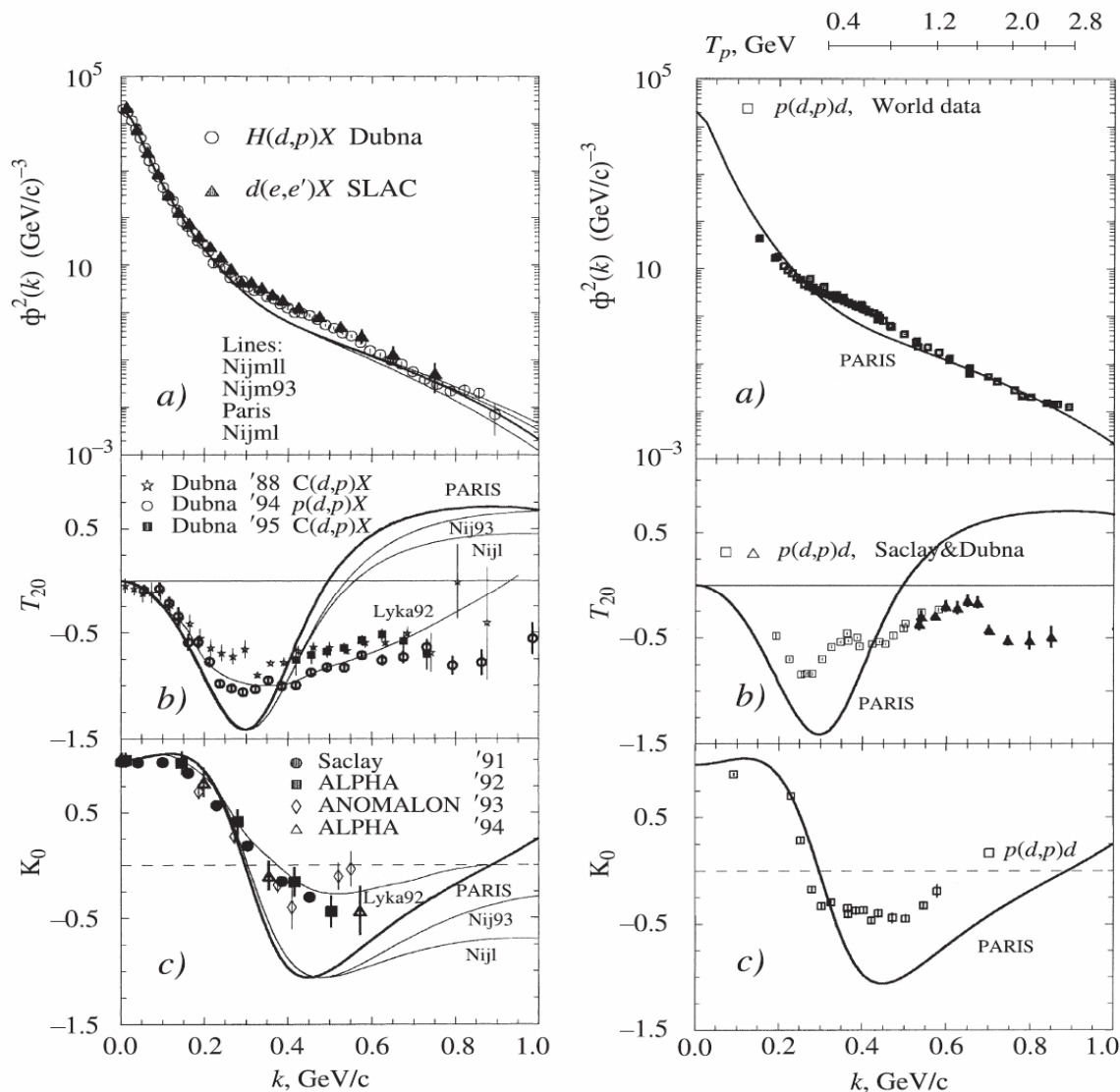
Рис. 5. Сводка данных экспериментов по фрагментации (слева) и упругому рассеянию «назад» (справа) поляризованных и неполяризованных дейтронов

Very nice phenomenological description of cross sections (using scale variables X) but huge problems to describe cumulative polarization phenomenons.

Where is the road to resolve problem of the nature of cumulative(subthreshold) particle production?

Do we see multiquark states inside nuclei or it's SRC of nucleons?

Which properties of these objects?

The first attempt to find answers
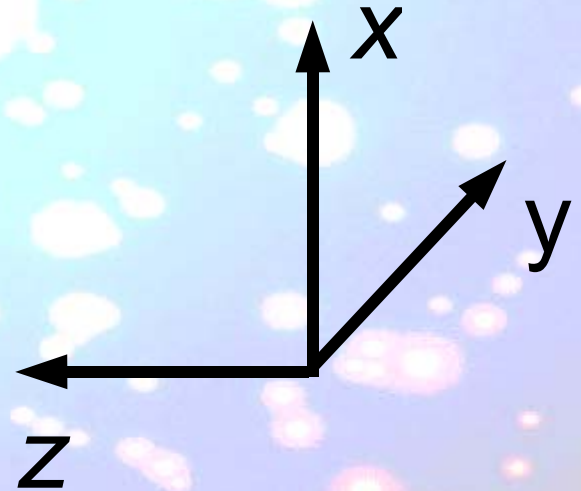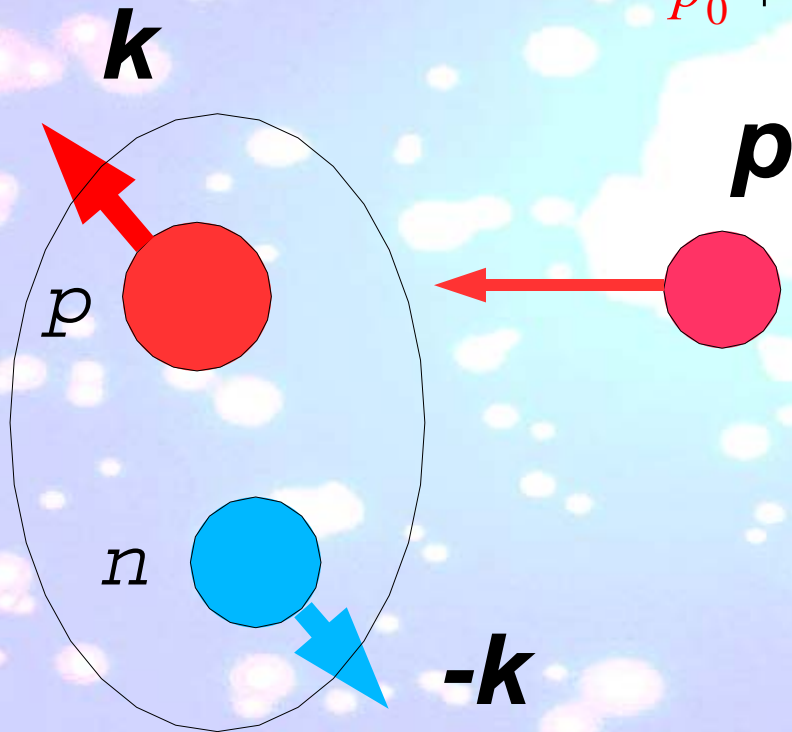
E850/EVA (BNL)
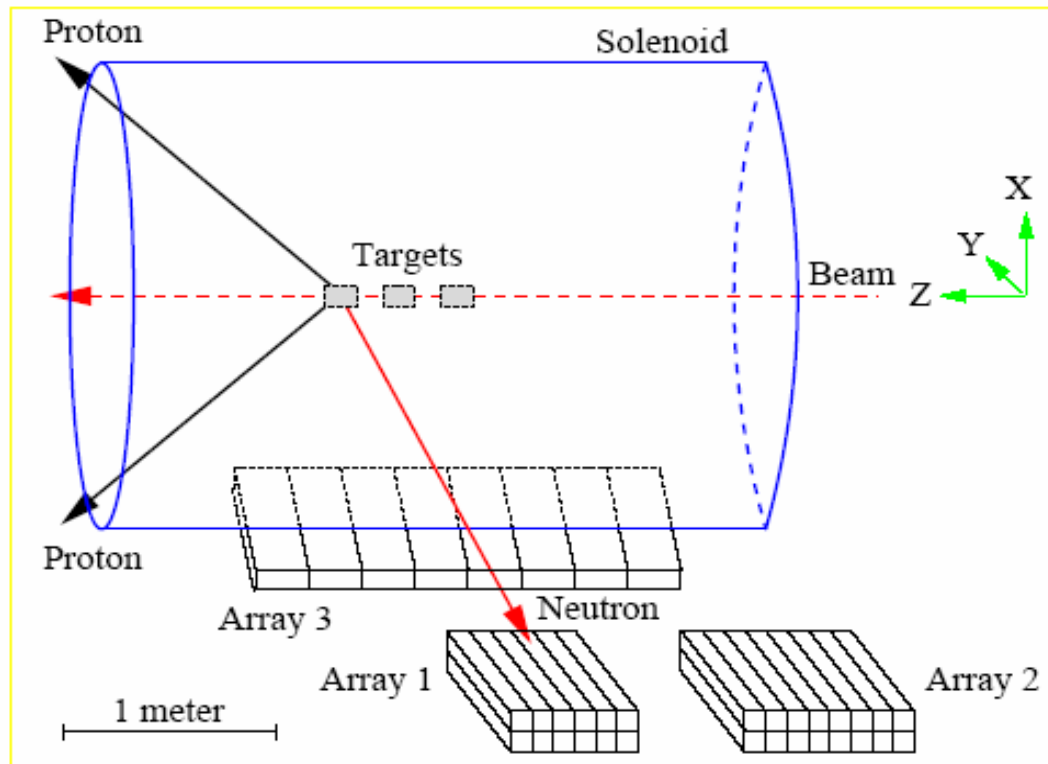
Figure I.3: A schematic view of the EVA solenoid and the neutron counters in the 1998 measurement.

n-p Short-Range Correlations from (p, 2p + n) Measurements

A. Tang,[1] J. W. Watson,[1] J. Aclander,[2] J. Alster,[2] G. Asryan,[4,3] Y. Averichev,[8] D. Barton,[4] V. Baturin,[6,5]
N. Bukhtoyarova,[4,5] A. Carroll,[4] S. Gushue,[4] S. Heppelmann,[6] A. Leksanov,[6] Y. Makdisi,[4] A. Malki,[2] E. Minina,[6]
I. Navon,[2] H. Nicholson,[7] A. Ogawa,[6] Yu. Panebratsev,[8] E. Piasetzky,[2] A. Schetkovsky,[6,5] S. Shimanskiy,[8] and
D. Zhalov[6]
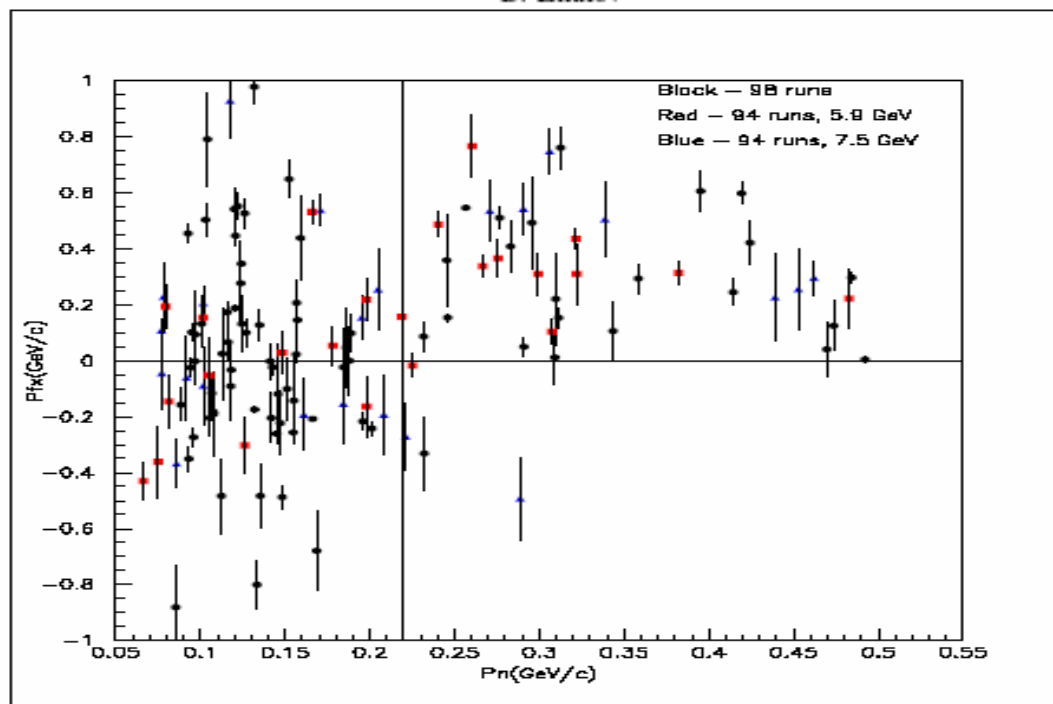
Figure I.5: The vertical component of the target nucleon momentum vs. the total neutron momentum. The positive vertical axis is the upward direction. The events shown are for triple coincidences of the neutron with the two high energy protons emerging from the QE C(p, 2p) reaction. The squares are for the 5.9 GeV/c incident beam and the triangles are for 7.5 GeV/c. The dots are preliminary unpublished data from the 1998 runing period. We associate the events in the upper right corner with NN SRC.

We need more complete investigation in the range of maximal p_T in semi-exclusive (and exclusive) experiment setup for comprehension of the nature of cumulative processes.
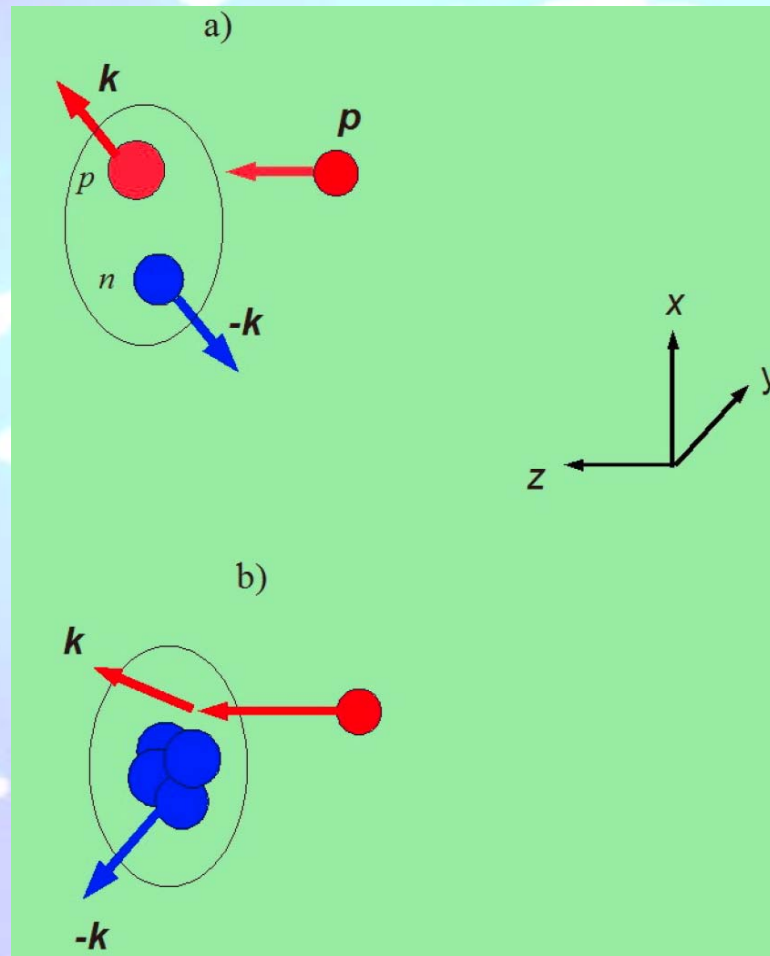
- average number of baryons accompanied high p_T cumulative particle producti... nd its $s_{cumulat}$ dependance;

- average multiplicity accompanied high p_T cumulative particle production and ...umulat dependance;

- $s_{cumulat}$ dependence of polarization characteristics (analyse power, asymmetry a... o on), for SRC mechanism will be scaling repeating effects for free nucleon-nucle... teractions;

- coincidence cross sections of high p_T cumulative particle production with pre... on of the "quark counting rules" [9] when using Stavinsky's variables.

Cumulative particle production pA collisions at 10 GeV/c
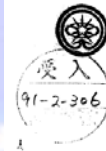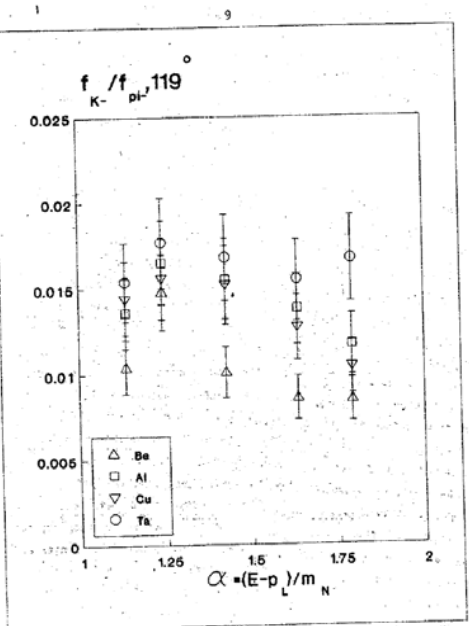
"The Horn"

Fig.5a. The ratio $R_-=f_{K^-}(\alpha)/f_{\pi^-}(\alpha)$ as a function of light cone variable $\alpha=(E-p_{\parallel})/m_N$.
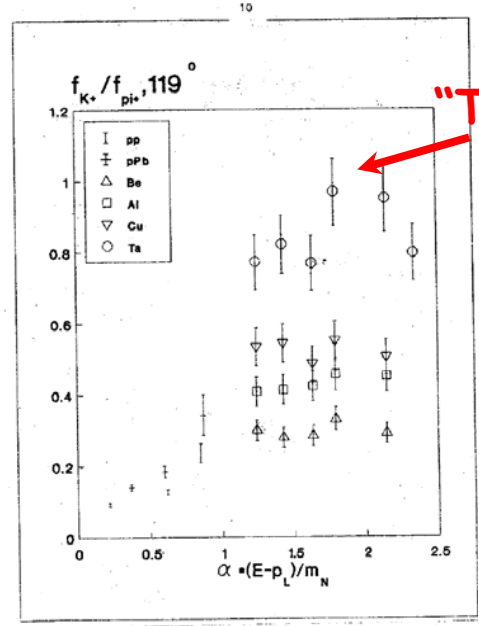
Fig.5b. The ratio $R_+=f_{K^+}(\alpha)/f_{\pi^+}(\alpha)$ as a function of light cone variable $\alpha=(E-p_{\parallel})/m_N$.

"The Horn"
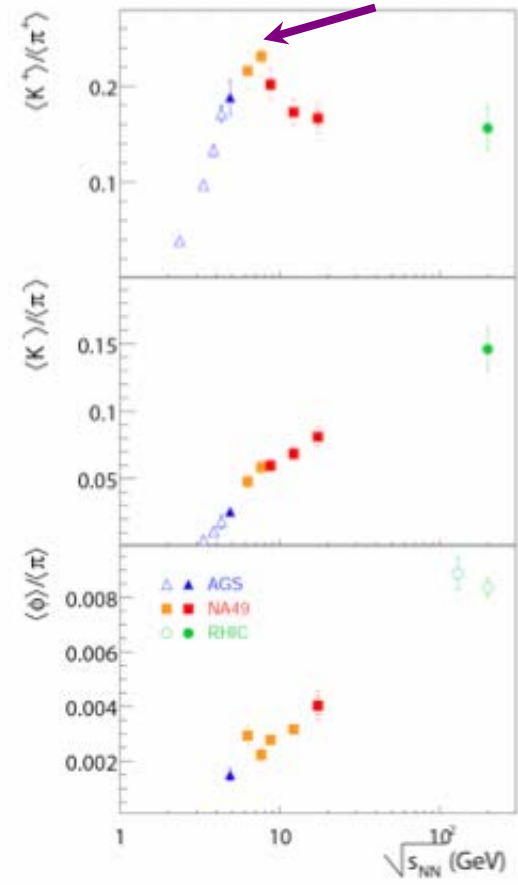
Non-monotonic behavior at AGS/SPS

NA49 Phys.Rev.C66:054902,2002

Plot from Claudia Hoehne, QM'05

The situation is very similar for cumulative(subthreshold) and high p_T processes where is very good description of cross sections(using constituent picture) and very bad understanding how to describe

polarization.

"Counting rules" and the phenomenology give us direction for future physical investigations.

Huge polarization effects (high p_T pp-collisions and s.o.) give additional tools.
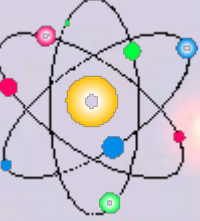
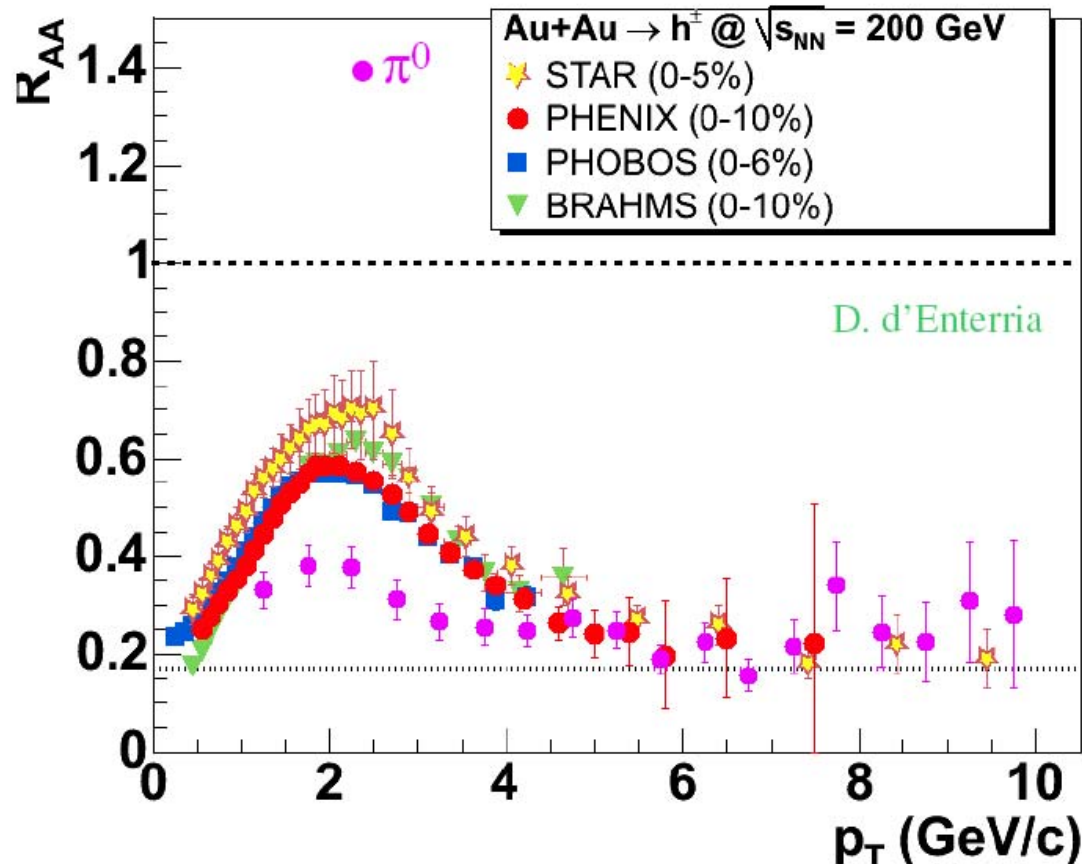# THANK YOU FOR ATTANTION!

Quark Gluon Plasma Physics

Johanna Stachel

Physikalisches Institut, Universität Heidelberg

CERN Summer Student Program - July 25 and 26, 2005

- Lecture I: Dense Matter and the Quark-Gluon Plasma

- Lecture II: Statistical Hadron Production

- Lecture III: Heavy Quarks and Jets as Probes of the QGP

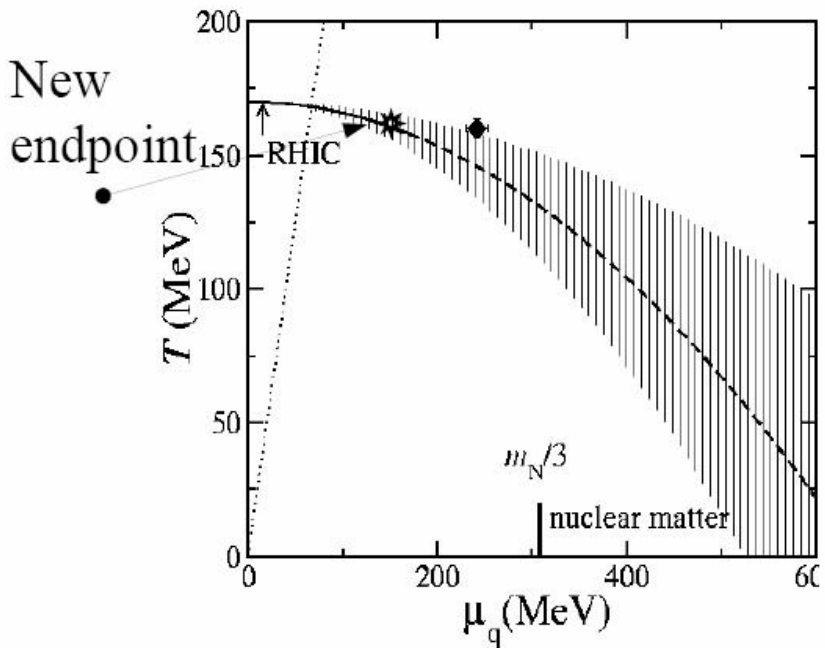Lectures assembled in collaboration with Peter Braun-Munzinger

high p_t suppression seen by all experiments

R_{AA}=yield(AuAu)/N_{coll} yield(pp)

$Au+Au \rightarrow h^{\pm}$ @ $\sqrt{s_{NN}}$ = 200 GeV
- STAR (0-5%)
- PHENIX (0-10%)
- PHOBOS (0-6%)
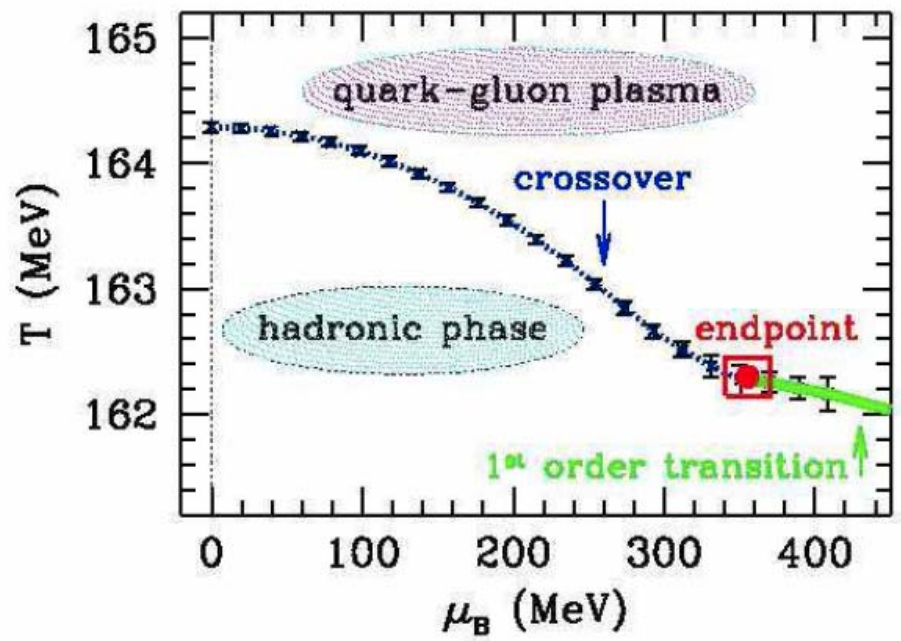- BRAHMS (0-10%)

π^0

D. d'Enterria

* all expts. see large suppression in AuAu
* π^0 lower than $h^{\pm}$
* no suppression in dAu rather
  Cronin enhancement
  $\rightarrow$ medium effect, not incoming partons

$\rightarrow$ reasonable agreement between 4 experiments

Johanna Stachel

RUPRECHT-KARLS-UNIVERSITÄT HEIDELBERG

Phase boundary from lattice QCD at finite baryon density

New endpoint

RHIC

T (MeV)

$m_N/3$

nuclear matter

μ_q(MeV)

S. Ejiri et al, hep-lat/0312006

quark-gluon plasma

crossover

T (MeV)

hadronic phase

endpoint

1st order transition

μ_B (MeV)

Z. Fodor, S. Katz, JHEP0404, (2004) 050

Note: $3\,\mu_q = \mu_B$

critical end point not (yet) well determined theoretically

With polarized ion beams we have real possibility to resolve many problems as are:

-"spin crisis"* of 70's (p↑p↑,p↑n↑,n↑n↑);

- color transparence (p↑A, p↑³He(d)↑);

-cumulative(subthreshold) particle production – to discovery the new state of nuclear Matter as "color quark condensate"
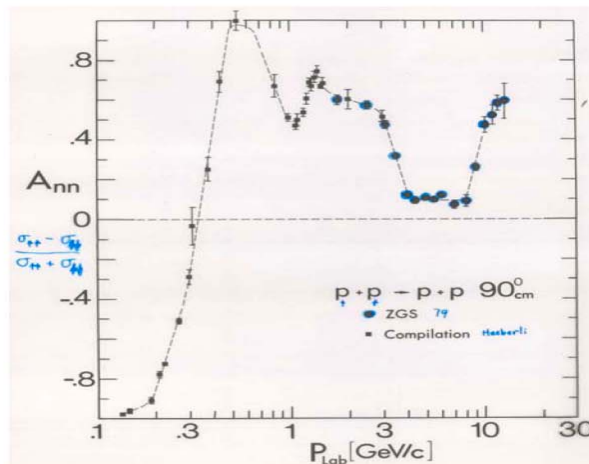
…

*) next slide

spin crisis" of 70's

Figure 4: A_{nn} is plotted against P_{Lab}.

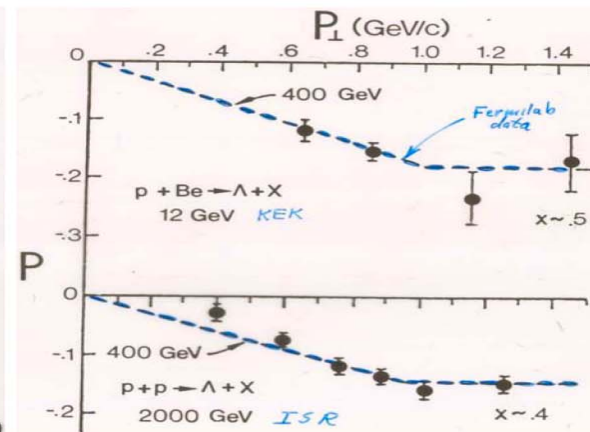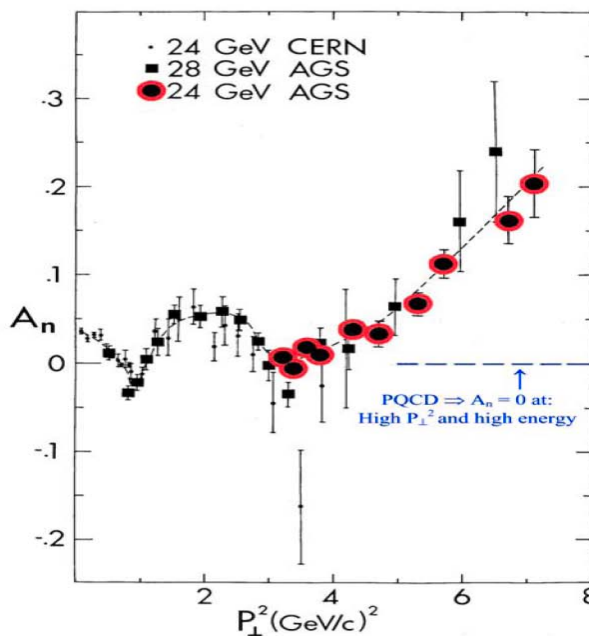Figure 6: The Λ polarization is plotted against P_t^2.
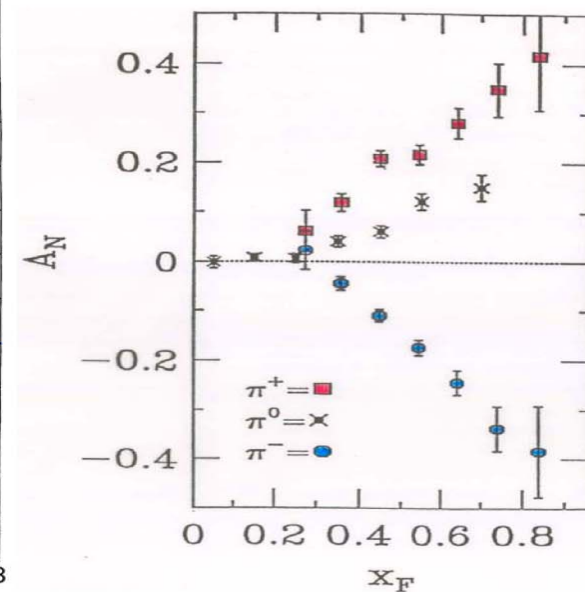

Figure 5: A_n is plotted against P_t^2.

Figure 7: A_n is plotted against X_F for inclusive π-meson production.